https://doi.org/10.5194/egusphere-2026-1024
Preprint. Discussion started: 10 June 2026

NUKLEUS - A First Kilometre Scale Multi-model Climate Ensemble for Germany: Evaluation

Kevin Sieck[1], Joaquim G. Pinto[2], Beate Geyer[3], Klaus Keuler[4], Christian Beier[4], Christoph Braun[2], Florian Ehmele[2], Hendrik Feldmann[2], Thomas Frisius[1], Philipp Heinrich[3], Marie Hundhausen[2], Ronny Petrik[3,5], and Katja Trachte[4]

[1]Climate Service Center Germany (GERICS), Helmholtz-Zentrum Hereon, Hamburg, Germany
[2]Institute of Meteorology and Climate Research – Troposphere Research (IMKTRO), Karlsruhe Institute of Technology (KIT), Karlsruhe, Germany
[3]Institute of Coastal Systems - Analysis and Modeling, Helmholtz-Zentrum Hereon, Geesthacht, Germany
[4]Chair of Atmospheric Processes, Brandenburg University of Technology (BTU) Cottbus-Senftenberg, Cottbus, Germany
[5]German Navy Headquarters, Rostock, Germany

Correspondence: Kevin Sieck (kevin.sieck@hereon.de)

Abstract. This study presents the evaluation of NUKLEUS, the first kilometre-scale, multi-model convection-permitting regional climate ensemble (CPM) for Germany. Three state-of-the-art regional climate models (ICON-CLM, COSMO-CLM, and REMO) were run at ~3 km horizontal resolution using a two-step downscaling chain driven by ERA5 reanalysis. The ensemble provides high-resolution climate information for Central Europe. In particular, we evaluate the CPM simulation results for Germany with a focus on six representative pilot regions selected within the German RegIKlim programme. Temperature, precipitation, global radiation, and near-surface wind, including their spatial patterns, annual and diurnal cycles, distributional characteristics, are compared to observational datasets. Moreover, selected climate indices relevant for heat and precipitation extremes are analysed. Overall, the ensemble demonstrates substantial added value compared to coarser-scale regional climate modelling, particularly in capturing regional climatic features and fine-scale variability. Temperature is reproduced with small biases (mostly within $\pm$ 0.5 K), with ICON-CLM performing best, while COSMO-CLM shows a weak cold bias and REMO a warm bias in parts of southern Germany. The CPM models realistically capture daily temperature distributions, though REMO underestimates minimum-temperature extremes. The annual cycle of precipitation is generally well represented, but all CPM models tend to overestimate totals in several regions, e.g., REMO exhibits a distinct spatial bias pattern with stronger deviations along topographic gradients. Extreme precipitation frequencies are generally overestimated, while regional contrasts such as stronger extremes in mountainous regions are preserved. Diurnal cycles show deficiencies specific to the models, including timing errors of afternoon precipitation peaks and misrepresentation of nocturnal precipitation revivals. For global radiation, ICON-CLM achieves the smallest biases, benefiting from its modern radiation scheme (ecRad), whereas COSMO-CLM and REMO show region specific over- and underestimations linked to cloud representation. 10 m wind speed diurnal cycles are best simulated by ICON-CLM, which captures the nocturnal wind minimum, while COSMO-CLM and REMO generally overestimate nighttime wind. Climate indices reveal underestimation of heat-related metrics (summer days and hot days) and systematic overestimation of heavy precipitation indices, although spatial patterns and regional differences are reproduced.

https://doi.org/10.5194/egusphere-2026-1024
Preprint. Discussion started: 10 June 2026

In summary, we conclude that NUKLEUS provides valuable climate information for Germany, supporting climate-impact assessments and adaptation planning at municipal to regional scales.

1 Introduction

The latest IPCC Assessment Report has provided further evidence that human-induced climate change is already in full swing, affecting precipitation, hot and cold extremes on most continents (Eyring et al., 2021). In addition to mitigating further warming, adapting to the ongoing changes will be one of the major challenges of the coming decades (Measham et al., 2011; Fünfgeld et al., 2023). In Germany, events such as the extreme drought of 2018 (Rousi et al., 2023) and the catastrophic Ahr Valley flood (Ludwig et al., 2023; Mohr et al., 2023) have intensified the urgency for action, particularly in the context of urban planning (Fünfgeld et al., 2026). Consequently, it is no longer sufficient to merely describe climate change and its impacts in a scientifically sound manner; the development and implementation of effective adaptation solutions have become essential. At the EU level, this is taken into account by the newly created EU Mission: Adaptation to Climate Change (Commission et al., 2021). In addition to research on climate risks, this mission aims to develop solutions for cities and municipalities in order to adapt to climate change.

As adaptation is mostly happening at regional to local scales, the demand for very high resolution climate information in order to support decision making is growing. To date, the data provided by global climate model (GCM) simulations is insufficiently resolved to satisfy this demand. However, recent advances in computer power and model development made regional kilometre-scale climate simulations feasible (Kendon et al., 2021; Lucas-Picher et al., 2021). Besides the pure technical feasibility of these simulations, they come with several advantages compared to coarser climate simulations in terms of the representation of physical processes (e.g., Prein et al., 2015; Coppola et al., 2018; Soares et al., 2024). One of the processes that has important societal impacts and can be better represented in detail is convective precipitation. In kilometre-scale climate simulations, convection is explicitly resolved in most models, which often leads to a much better representation of small-scale high-intensity precipitation events compared to models with coarser resolution. Recently, many studies have shown the often called “added value” of convection-permitting climate simulations compared to coarser resolved models. Large benefits are expected for the intensity distribution and diurnal cycle of precipitation (Lucas-Picher et al., 2021; Fowler et al., 2021; Hundhausen et al., 2024) due to the explicit treatment of convection. An added value has also been demonstrated for temperature (Soares et al., 2024; Hundhausen et al., 2023), near-surface wind speed (Molina et al., 2024), and for user-relevant climate indices (Pinto et al., 2026).

One of the challenges of convection-permitting climate simulations are the computational costs, especially when it comes to large ensembles that are needed to conduct proper uncertainty analysis. Currently, many activities with convection-permitting models are only carried out over time slices of 10 to 30 years and small domains by means of dynamical downscaling with regional climate models in the range of $1200\,\mathrm{km} \times 1200\,\mathrm{km}$. Only a few modelling groups are able to afford larger domains (e.g., Berthou et al., 2020) or small ensembles (Kendon et al., 2021; Hundhausen et al., 2023). Pioneering work is being done

https://doi.org/10.5194/egusphere-2026-1024
Preprint. Discussion started: 10 June 2026

in global convection-permitting simulations (e.g., Stevens et al., 2019). However, these models can only simulate a couple of months to a few years. Therefore, results from such models are currently not suitable for supporting climate change adaptation.

Another way to reduce computational costs is statistical downscaling or purely statistical methods, which under current climate conditions can often provide similar or better results than dynamical downscaling (e.g., Maraun et al., 2015; Gutiérrez et al., 2019). Two major challenges for statistical downscaling methods are the representation of future climate conditions due to the lack of training data, and the breakdown of the physical consistency between different variables, e.g., temperature and precipitation. Thus, statistical downscaling methods may have considerable shortcomings compared to other methods, particularly under strong climate change conditions, despite the benefit of lower computational costs (Lanzante et al., 2018). Hybrid statistical-dynamical downscaling methods aim to combine the advantages of statistical and dynamical methods. Such approaches may, however, be limited to specific variables (Reyers et al., 2015). A recently developed method is creating so-called "RCM emulators" (Doury et al., 2023). Despite promising results, this method is still under development and is not yet suitable for operational use.

Pioneering work in convection-permitting climate modelling was conducted in the framework of the World Climate Research Programme's Coordinated Regional Downscaling Experiments Flagship Pilot Study (WCRP CORDEX FPS; Giorgi et al., 2009; Gutowski Jr. et al., 2016) on convective phenomena at high resolution over Europe and the Mediterranean (Coppola et al., 2018) with the first decade long multi-model ensemble at convection-permitting scales for the Greater Alpine region. A major contribution to this FPS comes from the European Union funded European Climate Prediction system (EUCP; Hewitt and Lowe, 2018), which offers mini-ensembles with convection-permitting regional climate models for several other domains in Europe (EUCP Project Team, 2021).

In this study, we present the first multi-model convection-permitting regional climate model simulations for the entirety of Germany. Here, we will focus on the performance of the novel climate simulations for Germany at convection-permitting scales driven by ERA5 reanalysis data (Hersbach et al., 2020). The focus lies on the evaluation of basic meteorological variables in convection-permitting multi-model (CPM) simulations against observational datasets, namely temperature, precipitation, radiation, and wind speed. Additionally, selected climate indices are evaluated to cover the user perspective (Buontempo et al., 2018; Pinto et al., 2026).

The paper is structured as follows: Sect. 2 describes the modelling and evaluation strategy, introduces the CPM ensemble setup, and outlines the reference datasets and statistical methods used. Sect. 3 presents the evaluation results for temperature, precipitation, global radiation, wind speed, and selected climate indices across six pilot regions with special focus on two regions called 'East Frisia' and 'Thuringia, Saxony, and Saxony-Anhalt'. Results for the other pilot regions are given in the Supplementary Material. The discussion of model performance, regional differences, and implications for high-resolution climate information is provided in Sect. 4.

https://doi.org/10.5194/egusphere-2026-1024
Preprint. Discussion started: 10 June 2026

2 Method and Data

The CPM simulations were conducted within the NUKLEUS (Actionable local climate information for Germany) project, which is part of the funding measure RegIKlim (Regional climate information for climate action) of the German Federal Ministry of Research, Technology and Space. The RegIKlim program aims to create actionable knowledge for climate adaptation in Germany. Specifically, the basic concept focuses on six exemplary pilot regions, where partners from research, private companies, and administration at the municipality level create knowledge on how to handle challenges that arise from ongoing climate change. The six pilot regions were selected to ensure that the various landscape types representative of Germany were considered. These landscape types represent different local climates and face different challenges in adapting to climate change. Figure 1 shows the model domain indicating the six pilot regions: East Frisia (EF) representing a coastal area, Elbe-Elster (EE) characterizing a landscape water regime, a typical German low mountain region (Thuringia, Saxony, and Saxony-Anhalt; TSA), a Pre-Alpine region (PAR), and two pilot regions describing different types of urbanized areas with the city of Duisburg (DUI) and the area in and around the city of Stuttgart (STU). To streamline the needed climate information and create synergies between pilot regions, two cross-cutting projects were created. One of them is responsible for the overall coordination of the funding measure (WIRKSAM), while the other (NUKLEUS) is responsible for providing suitable climate information to the pilot regions and facilitating their effective use.

To meet of the user's demands in terms of climate information, several workshops with representatives of the pilot regions were conducted to create a simulation protocol for NUKLEUS. One important outcome was the need for climate information at the kilometre-scale in order to provide proper high resolution information at municipality level. Therefore, NUKLEUS ran climate simulations at convection-permitting scales (CPM simulations) with horizontal resolutions of about 3 km over a common Central European domain named CEU-3. Due to limited computational resources, the CPM simulations could only be done in time slices of 30 years. Given the available resources global warming levels following Vautard et al. (2014) were chosen instead of classical fixed time periods as representatives for mid- and end-of-century climate to maximize the user's benefit. As reference period 1961–1990 was chosen following the definition of the climate reference period by the World Meteorological Organization and Germany's National Meteorological Service (Deutscher Wetterdienst; DWD) (Kaspar et al., 2021). In addition to the reference and climate change simulations to be described in separate publications, evaluation simulations were performed, which downscale the ERA5 reanalysis data (Hersbach et al., 2020) over Europe for the period 2005–2014. Their quantitative analysis, presented by this publication, is intended to strengthen users' confidence in the chosen climate models and the quality of the provided climate data.

2.1 Model Description and Setup

The ERA5-driven CPM evaluation simulations were performed with the three different regional climate models (RCM) ICON-CLM, COSMO-CLM, and REMO, which have been widely used in the recent past with a particular focus on Central Europe. Two dynamical downscaling steps were used for each RCM. First, RCM simulations driven by three-hourly ERA5 reanalysis data were performed at a horizontal resolution at about 12 km on the so-called EURO-CORDEX domain (EUR-11, Fig. S1).

https://doi.org/10.5194/egusphere-2026-1024
Preprint. Discussion started: 10 June 2026

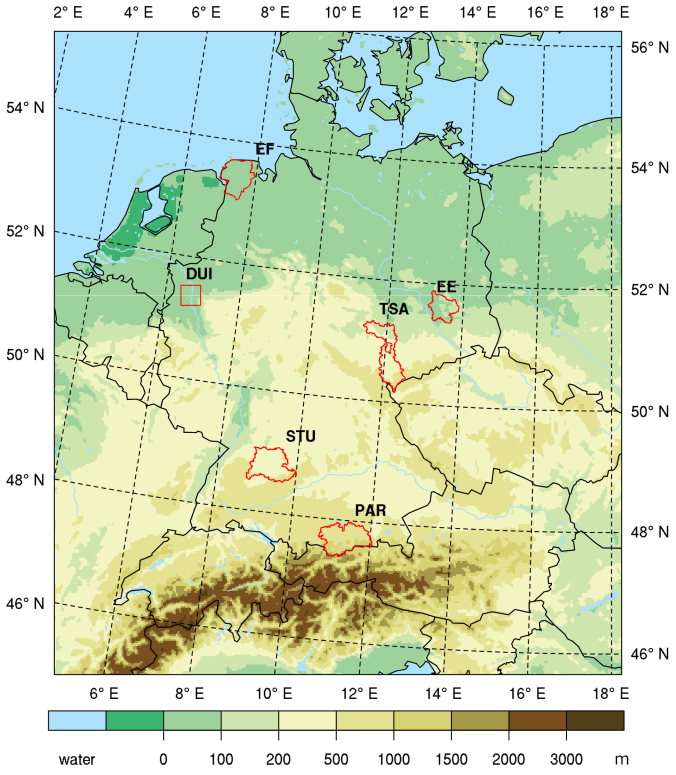

Figure 1. Central European domain (CEU-3) with selected pilot regions used for the statistical analysis of simulation results: coastal areas of East Frisia (EF), extended city areas of Duisburg (DUI) and Stuttgart (STU), Pre-Alpine region in South Bavaria (PAR), a county area in the border triangle of the federal states of Thuringia, Saxony and Saxony-Anhalt (TSA) and of the county Elbe-Elster (EE) in Southeast Germany.

The ERA5 product was provided by the European Centre for Medium-Range Weather Forecasts (ECMWF) and represents a detailed and realistic record of the global atmosphere and the land and ocean surface based on the Integrated Forecasting System (IFS Cy41r2; Hersbach et al., 2020). Second, these RCM simulations were used as initial and lateral boundary conditions to conduct CPM simulations at a horizontal grid resolution of about 3 km (CEU-3). This procedure aligns with the commonly used strategy for the Coordinated Regional Downscaling Experiments (CORDEX; Giorgi et al., 2009) for European climate simulations. While model domain, resolution, and simulation strategy were as similar as possible, each model used its own configuration for realizing the runs as described in the following subsections. In addition to different parametrizations of physical processes and numerical solution methods, this also concerned the specification of topography and other external fields, which primarily define soil and surface properties. Apart from the same horizontal resolution, the chosen RCMs use (slightly) different structured grids (see below). Hence, the results of the CEU-3 CPM simulations are prepared for a common grid in regular rotated coordinates with a grid spacing of 0.0275 °, which is identical to the COSMO-CLM and REMO grid and shown in Figure 1.

https://doi.org/10.5194/egusphere-2026-1024
Preprint. Discussion started: 10 June 2026

2.1.1 ICON-CLM

The modelling framework ICON (Zängl et al., 2015) was originally developed for a wide range of spatial and temporal scales and is used for global climate simulations (Giorgetta et al., 2018), numerical weather prediction (NWP), and large-eddy simulations (LES; Heinze et al., 2017). NWP and LES applications include a limited area version (ICON-LAM) of the global ICON code. Based on ICON-LAM with the NWP physic package, Van Pham et al. (2021) have developed a regional climate version (ICON-CLM) suitable for transient long-term regional simulations with time dependent lateral boundary conditions and resolutions between 50 km and 1 km. The transformation of the NWP version towards a regional climate version required several modifications and extensions of the original code, like a flexible temporal update of sea surface temperature, sea-ice cover, and greenhouse gas concentrations in preselected intervals from external data files, a variable configuration of the number and individual depths of soil layers, controllable output intervals for accumulated quantities including a reset option, adjustment of the lateral boundary treatment if cloud liquid water content and cloud ice content are missing in the driving GCM data, and calculations of additional diagnostic output fields.

ICON simulations are executed on unstructured triangular grids that originate from a spherical icosahedron with 20 equal-sized triangles, which can be stepwise refined by halving the size of the nested triangles (Prill et al., 2023). The temporal integration of the non-hydrostatic set of model equations is done by using an explicit two-time-level predictor-corrector scheme and a time splitting with additional sub-steps per dynamic time step for terms describing the propagation of sound-waves, which is implicitly solved (Zängl et al., 2015). The transport of tracers like the various water substances is based on a finite volume discretization, uses a directional splitting between vertical and horizontal components, and is solved by a cell-integrated semi-Lagrangian scheme (Prill et al., 2023), which uses a precalculation of the tracer's trajectory and conserves the mass flow between neighbouring grid cells. Further details of the model dynamics can be found in Zängl et al. (2015)

The parameterization of physical processes in ICON-CLM is close to the NWP configuration used at the DWD for operational weather forecasts. Radiation transfer is solved by the ecRad scheme (Hogan and Bozzo, 2018), which was originally developed by ECMWF for its Integrated Forecasting System (IFS) and uses aerosol optical properties and greenhouse gas concentration from external files. Cloud microphysics are calculated with the single-moment scheme of Seifert (2008) as described in Doms et al. (2021), using a three-category ice scheme with cloud ice, snow, and graupel. Deep, mid-level, and shallow convection on the sub-grid scale are parametrized by the Tiedtke/Bechtold scheme (Tiedtke, 1989; Bechtold et al., 2008), whose underlying parametrization according to Tiedtke (1989) is the same as in COSMO-CLM. The extension by Bechtold et al. (2008) offers a substantial improvement, which is particularly reflected in a better representation of the diurnal cycle of convective precipitation. In the CPM simulations at 3 km resolution, deep and mid-level convection are switched off, so that only the shallow convection part remains. The parameterization of vertical turbulent transfer according to Raschendorfer (2008) is based on a prognostic TKE equation and is the same as used in the COSMO-CLM simulations. Land surface and soil processes are treated in an own sub-module TERRA-ML (Schrodin and Heise, 2001; Schulz et al., 2016) in combination with the lake model Flake of Mironov (2008) and a sea-ice parameterization scheme developed by Mironov et al. (2012). The TERRA-ML version used by ICON is similar to that of COSMO-CLM with one substantial difference. ICON-CLM includes a tile approach,

https://doi.org/10.5194/egusphere-2026-1024
Preprint. Discussion started: 10 June 2026

which enables the consideration of various surface types within one grid-cell. Soil and surface parameterizations are calculated separately for each tile before the final surface fluxes are weighted averaged over the different tiles. The ICON-CLM simulations run with three tiles representing the three largest land use fractions by area per grid cell. Furthermore, parameterizations for non-orographic gravity wave drag, sub-grid scale orographic drag, and cloud cover are included (for more details see Prill et al., 2023).

The ICON-CLM simulations for this study are based on ICON version 2.6.5. They are executed on the icosahedral grid R3B7 (Zängl et al., 2015) with 162,452 grid cells for the Central European domain. The effective mesh size of the triangular grid is about 3 km and therefore comparable with that of the other two regional models operating on a regular rotated latitude-longitude grid. For a more practical handling, an easier comparison with COSMO-CLM and REMO results, and the common publication in the Earth System Grid Federation (ESGF) data archive, the ICON output is interpolated (by means of nearest neighbour) to the same regular target grid CEU-3 in rotated coordinates as used by the other two models and indicated in Fig. 1. The entire model domain covers more than 15 additional grid rows on each side of the target grid. This outer grid zone contains a 14 cell rows wide boundary and nudging zone (see chapter 6.2 in Prill et al., 2023) where the forcing data of the driving models are interpolated and relaxed to the regional ICON grid.

The basic time steps used for tracer transport and the fast-physics parameterizations is 25 s. The dynamical core solving the wave propagation uses a five times smaller time step. The time steps for slow physics are individually increased by a factor of 3 for convection and cloud cover calculations, a factor of 6 for sub-grid scale orographic drag and non-orographic gravity wave drag effects, and by a factor of 9 for radiation. Furthermore, the radiative transfer is calculated on a reduced "parent grid" with half the resolution of the model grid itself.

Soil processes are resolved by eight non-equidistant layers with tripling layer thickness from 0.01 m at the top to 14.58 m in the lowest layer, which leads to an overall soil depth of 21.87 m. However, hydrological processes are dynamically solved only in the upper six layers. The ERA5 driven evaluation runs did not use any spin-up procedure for the soil, in contrast to the COSMO-CLM and REMO simulations, as the critical soil moisture index, required for the soil initialization, is directly provided by the reanalysis data. The initial state of the soil in the CPM runs is directly interpolated from the coarser grid of the transient RCM simulation, as both resolutions use the same vertical soil structure and soil moisture index can be adequately transferred to the individual soil conditions of each finer grid cell.

2.1.2 COSMO-CLM

COSMO-CLM (CCLM; Rockel et al., 2008) is the climate version of the COSMO model (Baldauf et al., 2011), a limited-area and non-hydrostatic numerical weather prediction model developed by the DWD. It is maintained by the CLM-Community COSMO-CLM and the model version used in this study is COSMO6.0_clm1 published in 2021. For temporal integration a two-time-level, third-order Runge–Kutta scheme is used. The horizontal advection of wind components is performed with a fifth-order upwind scheme, and the vertical advection is performed by a third-order implicit advection. Scalars are transported using a second-order Bott advection scheme with deformational correction. Fast processes were treated by the newest version of the fast waves solver by Baldauf (2013) and Doms et al. (2021). More details about the COSMO model configuration of

https://doi.org/10.5194/egusphere-2026-1024
Preprint. Discussion started: 10 June 2026

dynamics can be found in Baldauf et al. (2011). Regarding the parameterization of physical processes, model configuration is close to the NWP configuration (Baldauf et al., 2011), but adapted to follow the recommendations of the CLM-Community. For example, the albedo is chosen to be dependent also on the soil moisture, in order to capture appropriately the feedback between soil and near-surface temperatures (large albedo values for dry soil and reduced albedo for wet soil). The type of root distribution is not uniform but follows an exponential decay. The calculation of heat conductivity considers not only soil moisture but also soil ice. The parameterization of bare soil evaporation follows a resistance approach aiming at an improved representation of evaporation fluxes under dry and wet conditions compared to the older parameterizations (Schulz and Vogel, 2020).

The model domain used for COSMO-CLM consist of 385 by 425 grid cells which exceeds the common CEU-3 grid by 20 pixel at each side including a lateral sponge zone of 10 grid lines. In vertical direction, COSMO-CLM utilizes 55 terrain-following levels with geometric height coordinate.

The CPM simulations were performed using ten non-equidistant soil layers with a thickness ranging from 10 cm near the surface to about 7.6 m in the deeper soil. Regarding the initialization of the soil properties, a preprocessor was used to transfer the values from the EUR-12 grid to the CEU-3 grid. The procedure for the soil moisture follows the concept of the soil moisture index as used also for ICON-CLM. The soil temperature is treated by linear interpolation. Finally, the spin-up time for the soil on the CPM grid was specified to be 3 months.

2.1.3 REMO

The original regional climate model REMO (Jacob and Podzun, 1997) is a hydrostatic limited-area model of the atmosphere that has been developed for many years. In recent years, an extension with a non-hydrostatic option (REMO-NH) originally developed by Göttel (2009) following Janjic et al. (2001) has been re-implemented to allow for climate simulations at convection-permitting scales. The current version REMO2020 has a unified dynamical core that allows running REMO and REMO-NH from the same code base. It is described by Pietikäinen et al. (2025) in detail. We will only briefly summarize the configuration of the 3 km climate simulations used here.

For the 3 km NUKLEUS ensemble, REMO-NH was used with a leap-frog time integration and Robert–Asselin–Williams filtering (Williams, 2009). The relaxation scheme of Davies (1976) for the boundary conditions is employed for the prognostic variables surface air pressure, horizontal wind components, air temperature, specific humidity, cloud liquid water, and cloud ice. For the additional prognostic variables, such as vertical non-hydrostatic pressure, vertical velocity, rain and snow hydrostatic conditions respectively, zero flux is prescribed at the boundaries. In the vertical, 49 hybrid sigma pressure levels were used for integration with a model top at 20 hPa. Only shallow convection is parametrized. For the surface processes, the REMO2020 standard setup with a tile approach surface scheme distinguishing between land, water, and ice fractions was used. For inland water bodies, FLake (Mironov, 2008), and for ocean prescribed sea surface temperatures from the forcing model were used.

The Initial conditions for the soil variables are taken from an earlier simulation conducted within the EUCP project (Hewitt and Lowe, 2018) using ERA-Interim (Dee et al., 2011) as boundary conditions. We do not expect large differences in the deep soil state using different reanalysis products as boundary conditions. In addition, the implementation of the soil and its

https://doi.org/10.5194/egusphere-2026-1024
Preprint. Discussion started: 10 June 2026

properties are identical between the model version used here and the earlier EUCP simulations. Nevertheless, we performed a one year spin-up to get as close as possible to an equilibrium state at initialization.

2.2 Reference data

The evaluation of the CEU-3 simulations requires reference data of adequate quality and sufficiently high horizontal resolution. Therefore, we chose the HYRAS data set v5.0 of DWD (Rauthe et al., 2013; Razafimaharo et al., 2020) as the main reference. This data set provides daily values of mean, maximum, and minimum temperature, near-surface relative humidity, and surface downwelling solar radiation on a regular 5 km grid with a Lambert conformal conic projection. In addition, daily precipitation values are available with a horizontal resolution of 1 km. As the HYRAS data set does not provide sub-daily temporal resolution, the RADKLIM data set provided by DWD (Winterrath et al., 2018) was additionally used to analyse the diurnal cycle of precipitation. It is a radar-based precipitation climatology for Germany at high resolution in space (1 km) and with a frequency of one hour. RADKLIM was dedicated for qualitative analysis of short-duration precipitation events, but it is inherently biased with respect to precipitation amounts: Hänsler and Weiler (2022) showed underestimation of convective precipitation, and Hammoudeh et al. (2025) found biases of up to -25 % for the seasonal and annual sums (see Figure 3 in their publication). Similarly, Hundhausen et al. (2025) found an underestimation of hourly to sub-hourly precipitation extremes in RADKLIM data compared to station observations. Therefore, RADKLIM was only used for qualitative analysis of the daily cycle, while for all other precipitation analyses HYRAS is used.

For the validation of wind speed and temperature, we use the hourly data from the Test Reference Years (TRY) data set by Krähenmann et al. (2016). It is a high-resolution gridded data set ($1 \times 1\,\mathrm{km}^2$) of hourly meteorological variables for Germany, which are available for 1995–2012. The gridded data were derived from synoptic station data provided by DWD, supplemented by satellite observations (CM-SAF) and model data regarding wind speed (COSMO-CLM).

To analyse global radiation, we use the SARAH-3 data set (Pfeifroth et al., 2023). It is a climate data record of surface solar radiation parameters based on data from the MVIRI and SEVIRI sensors onboard the METEOSAT satellite series. The high-resolution data with 0.05 ° and 30 minutes were interpolated to the model resolution in time and space. We also use station data from DWD (Kaspar et al., 2013) for comparison. The number of available stations in the six pilot regions is as follows: EF (4), DUI (5), STU (18), PAR (9), TSA (18), EE (7).

2.3 Statistical analysis

A basic overview of the quality of the CPM simulations is given by two-dimensional bias plots. Furthermore, mean annual cycles are presented as spatial averages over the selected pilot regions (see Fig. 1). The distances between the simulated annual cycles and the reference data are quantified by the mean bias (MB) and the mean absolute difference (MAD). For both metrics, the ten-year monthly means of a simulation and the reference data are first calculated at grid-point level and then spatially averaged over all grid cells of a pilot region. Subsequently, the monthly values of MB and MAD are arithmetically averaged. Thus, the MB also reflects the bias of the climatological annual mean values of a pilot region.

https://doi.org/10.5194/egusphere-2026-1024
Preprint. Discussion started: 10 June 2026

As further statistical measure, frequency distributions are presented as approximated curves of the empirical probability density function (PDF curves) for all pilot regions. The overlap between the two PDF curves of the simulated and the reference data is quantified by the Perkins skill score (PSS; Perkins et al., 2007)). Additionally, the mean absolute quantile difference (MAQD) is calculated. This metric measures the absolute deviation between the cumulative probability density functions of the simulated and the reference data based on quantiles for the p-values 0.001, 0.005, 0.01, 0.05, 0.1, ..., 0.9, 0.95, 0.99, 0.995, 0.999.

Additionally, we present diurnal cycles as absolute values and their biases to observations for the summer months June and July for $2\,\mathrm{m}$ temperature, radiation, $10\,\mathrm{m}$ wind speed, and precipitation with the time given in UTC. For quantification, we calculate the mean absolute hourly difference (MAHD) for radiation, the ratio in the diurnal temperature range (RDTR) for the $2\,\mathrm{m}$ temperature with values near 1, where values greater 1 indicate an overestimation of the diurnal temperature range, and the rank correlation coefficient of mean hourly values for precipitation and $10\,\mathrm{m}$ wind speed.

To avoid an influence of different grid resolutions between CPM simulations and reference data in the spatial bias plots, HYRAS data were regridded for precipitation from the HYRAS $1\,\mathrm{km}$ grid to the CEU-3 grid using a conservative method of the Climate Data Operator routines (Schulzweida, 2022). All other variables are regridded from the HYRAS $5\,\mathrm{km}$ grid to the CEU-3 grid with nearest neighbour remapping (Schulzweida, 2022) and, in the case of temperature, a height correction of $0.0065\,\mathrm{K\,m^{-1}}$ was applied. The frequency distributions and mean annual or diurnal cycles are, however, calculated on the original grids in order to avoid a flattening of extreme grid values by any remapping procedure.

2.4 Climate Indices

We analyse descriptive indices of extremes based on the core set of 27 indices of extremes defined by the Joint CCl/CLIVAR/JCOMM Expert Team on Climate Change Detection and Indices (ETCCDI, 2014) and Alexander and Herold (2016). In this study, we focus on a subset of five indices to assess heat stress, cold stress, and extreme precipitation (Table 1). For temperature, we consider threshold-based indices of the annual number of summer days (SU), the number of hot days (HD) and the number of frost days (FD). To assess precipitation extremes, we use the contribution of very wet days to annual wet-day precipitation (R95ptot), as well as the annual number of very heavy rain days (R20mm). The definitions are provided in Table 1. Such indices have been utilised in several studies focussing on climate change adaptation for Europe (Buontempo et al., 2018; Pinto et al., 2026)

Please note that the formulation used here with strict inequalities (“larger (smaller) than”) is slightly from the formulations used by the German Weather Service, which are formulated as inclusive inequalities (“larger (smaller) or equal than”; cf. Pinto et al. (2026)). All climate indices are calculated from the simulations on the common CEU-3 grid and remapped HYRAS data on the CEU-3 gird as described above, using the Freva plugin ClimDexCalc2 (Kadow et al., 2021) based on the package ClimPACT (Alexander and Herold, 2016).

https://doi.org/10.5194/egusphere-2026-1024
Preprint. Discussion started: 10 June 2026

Table 1. Overview of selected climate indices. TX_{ij}: daily maximum temperature, TN_{ij}: daily minimum temperature of day i in year j. $TX_{in}90$ and $TN_{in}90$: 90th percentile. RR_{wj}: daily precipitation amount of wet days w ($\geq$ 1mm) in year j, W: number of wet days in j, RR_{ij}: daily precipitation amount on day i in year j, $RR_{wn}95$: 95th percentile on wet days. The definition of the indices is based on ETCCDI (2014) and Alexander and Herold (2016)

Climate indices	Abbreviation	Unit	Calculation
Summer days	SU	days	$TX_{ij} > +25\,^{\circ}\mathrm{C}$
Hot days	HD	days	$TX_{ij} > +30\,^{\circ}\mathrm{C}$
Frost days	FD	days	$TN_{ij} < 0\,^{\circ}\mathrm{C}$
Contribution from very wet days	R95ptot	%	$\frac{\sum_{w=1}^{W} RR_{wj}}{\sum_{i=1}^{I} RR_{ij}}$ where $RR_{wj} > RR_{wn}95$
Very heavy rain days	R20mm	days	$RR_{ij} \geq 20\,\mathrm{mm}$

3 Evaluation results of CPM simulations

The following subsections presents the basic evaluation results for 2 m temperature, precipitation, global radiation, and 10 m wind speed, as well as selected climate indices. The latter are: number of summer days (SU), number of hot days (HD), number of frost days (FD), precipitation from very wet days (R95ptot), number of days with very heavy rain (R20mm), as described in the previous section. All figures and metrics are prepared as "climatological" quantities for the ten-year simulation period 2005–2014 of the CPM evaluation runs on CEU-3. An exception is the evaluation of the diurnal cycles of temperature and wind. Only 8-year averages are considered here, as hourly TRY data are only available until 2012. The main part of the paper presents figures only for two of the six pilot regions, namely EF and TSA, but discusses results from other regions, too, if worth mentioning. The corresponding figures are shifted to the supplemental material for the sake of succinctness.

3.1 Temperature

Figure 2 shows the bias of the ten-year annual mean of the 2 m daily mean temperature for the three CPM simulations with respect to the HYRAS reference data. In most regions, the deviations are within the range of ± 0.5 K. ICON-CLM shows the smallest deviations overall in annual mean. CCLM tends to slightly colder temperatures, particularly in northern Germany, while REMO generally generates up to 1 K higher temperatures in southern Germany than the reference. Despite the differences in the absolute values, the bias shows a similar spatial structure in all three simulations with smaller or negative deviations in the north and larger or positive deviations in the south.

The annual cycles of the simulated ten-year monthly mean temperatures, shown in Fig. 3 for the EF and TSA regions, are within the range of the observation stations of the respective region. The spread of observations is larger in TSA than in EF

https://doi.org/10.5194/egusphere-2026-1024
Preprint. Discussion started: 10 June 2026

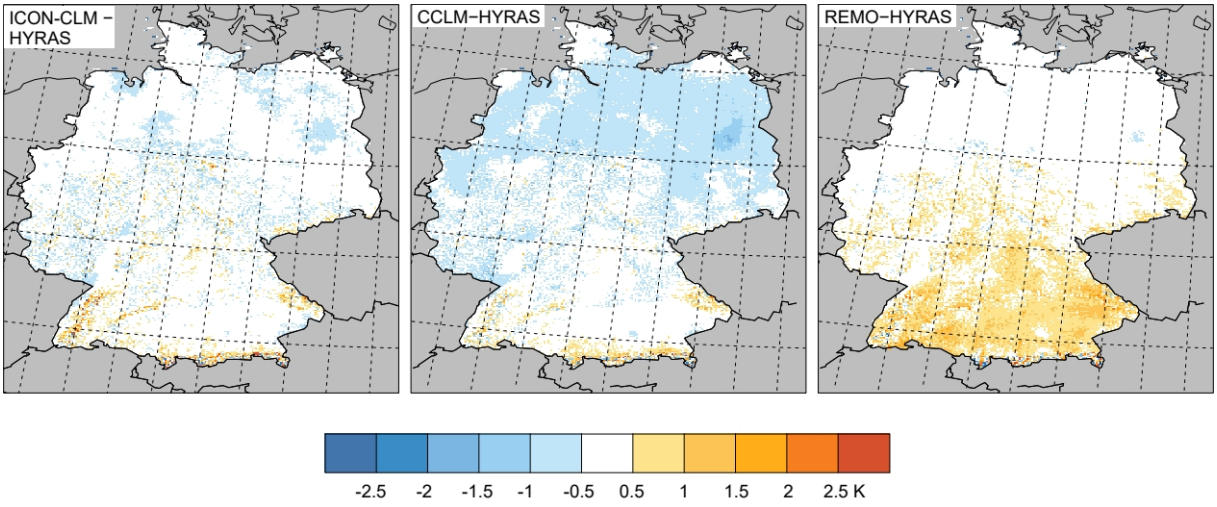

Figure 2. Bias of the annual mean 2 m temperature in Kelvin on CEU-3 for the period 2005–2014 and the three CPM simulations with ICON-CLM, CCLM and REMO with respect to HYRAS reference data.

because of the greater variation in orography (and the larger number of reference stations) in the TSA region than in the much flatter EF region.

ICON-CLM and CCLM have a negative bias of up to -0.8 K in both regions and almost all months, which is lower in summer than in winter and tends to be a few tenths of a degree weaker in ICON-CLM than in CCLM. The REMO simulation also shows generally higher temperatures here, leading to weakly negative to slightly positive deviations in EF and to a generally positive bias of up to 1.5 K in TSA. Overall, the variation of the monthly bias over the year appears to be stronger in REMO than in the other two simulations. The monthly bias has a substantially different shape in the PAR region (see Fig. S2 in the Supplementary Material), which also has the strongest spread in the observation data. Here, the winter months have a generally positive bias of up to 1.5 K, while the summer months show much weaker positive to slightly negative deviations.

The temperature deviations between the simulations and the reference data are objectively quantified by the MB and MAD presented in Fig. 4. Identical absolute values of the two metrics mean that all 12 monthly deviations have the same sign. This is the case, for example, with 0.37 K and 0.41 K in the EF pilot region in the ICON-CLM and CCLM simulations. The REMO simulation shows alternating signs for the monthly bias in all pilot regions. An MB close to zero (region STU in ICON-CLM and CCLM, EF in REMO) indicates that the individual monthly deviations almost compensate each other over the year to a nearly perfect annual mean. In general, the monthly deviations are very moderate and well below 1 K in the annual average for all pilot regions. The largest absolute deviations occur in the simulations with ICON-CLM (0.41 K) and CCLM (0.72 K) for the DUI region and in the REMO simulation (0.65 K) for the STU region. Even the topographically complex PAR region only shows absolute deviations between 0.28 K (ICON-CLM) and 0.55 K (CCLM).

https://doi.org/10.5194/egusphere-2026-1024
Preprint. Discussion started: 10 June 2026

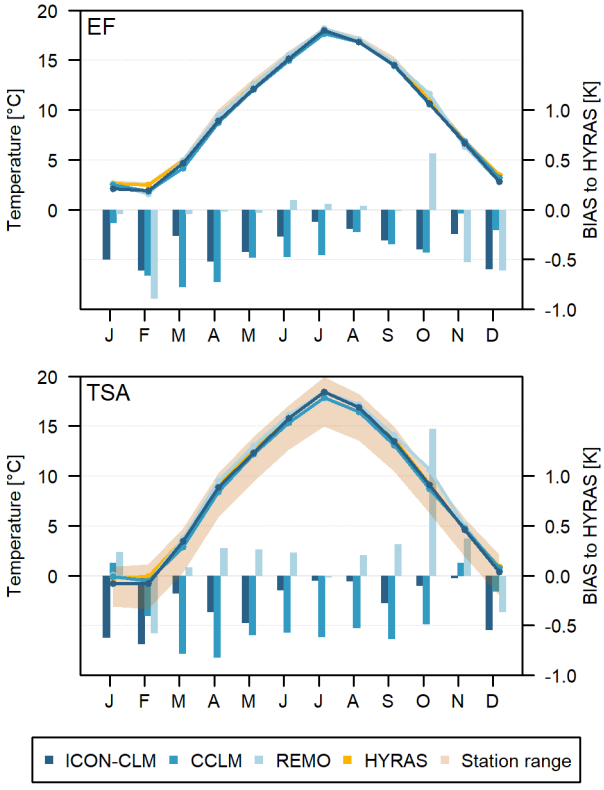

Figure 3. Annual cycle of monthly mean temperature (curves, left axis) and temperature bias (shaded bars, right axis) for the period 2005–2014 and the three CPM simulations on CEU-3 with ICON-CLM (dark blue), CCLM (blue) and REMO (light blue) against HYRAS reference data (dark yellow curve) averaged over the pilot regions EF (upper panel) and TSA (lower panel). The ochre-coloured range represents the span of corresponding values from station observations located within the respective pilot region.

The frequency distributions of the simulated daily maximum temperatures (Tmax), presented as the probability density function (PDF) in Fig. 5, generally agree quite well with those of the reference data and observation stations. REMO tends to underestimate the mean temperature range but captures the higher temperature values better than CCLM and ICON-CLM.

As shown by the PSS in Fig. 6, the overlap of the PDFs is mostly above 0.94 with a minimum of 0.9 in the CCLM simulation for the EE region. While the PSS primarily captures deviations in the middle range of the PDF, the MAQD reacts more sensitive to deviations in the extreme percentiles for high and low p-values. The lower MAQD values in the REMO simulation reflect the better detection of high percentiles in all six pilot regions. The largest deviations of 1.35 K occur in the PAR region of the CCLM simulation (see also Fig. S9 in the Supplementary Material).

The overlap of the PDFs for the daily minimum temperature (Tmin) in Fig. 7 is comparable to or slightly better than the overlap of Tmax frequencies for ICON-CLM and CCLM. For REMO it is slightly worse as a comparison of PSS in Fig. 8 (with values down to 0.86) with that in Figure 6 indicates. Reasons are a substantial accumulation of values around freezing

https://doi.org/10.5194/egusphere-2026-1024
Preprint. Discussion started: 10 June 2026

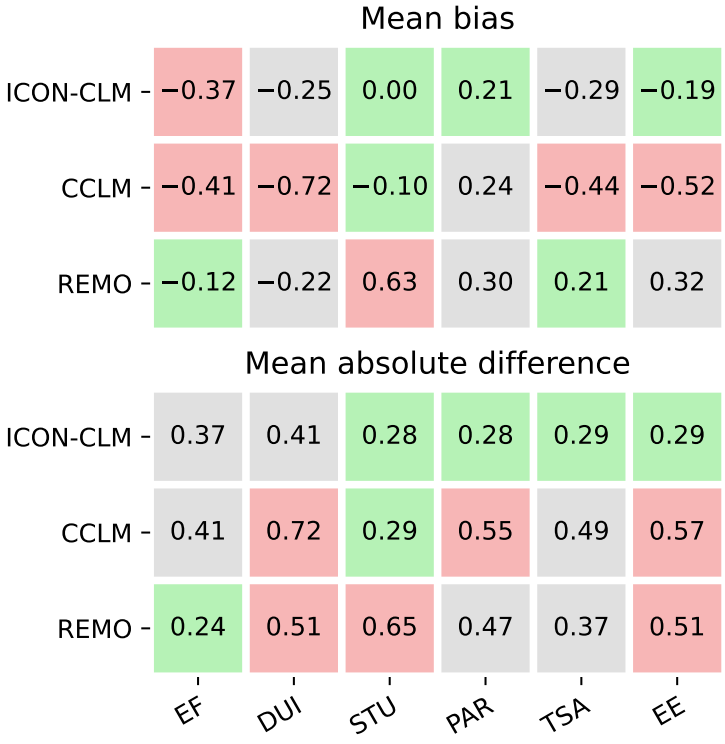

Figure 4. Mean bias and mean absolute difference of monthly mean temperatures in Kelvin with respect to HYRAS for all pilot regions and simulations. For a first qualitative assessment, the range of values spanned by the models is divided into three categories (terciles): green highlighted cells represent the best tercile, red the worst, grey cells lie in between.

point and a shift to higher temperatures, in general, resulting in an underestimation of values in a wide range below zero and an overestimation of high minimum temperatures compared to the simulations with ICON-CLM and CCLM. The somewhat poorer reproduction of extreme minimum temperatures in the REMO simulation is also reflected in the higher MAQDs in Fig. 8 with values up to 2.26 K for the PAR pilot region.

The diurnal cycle for temperature is best depicted by the ICON-CLM (see Fig. 9). In contrast, COSMO-CLM and, to some extent, REMO suffer from a decay too early in the afternoon, which is pronounced for the TSA region and leads to a BIAS of -1 K in the late afternoon (see Fig. 9). The REMO simulation offers an overestimation of night temperatures and warming during the morning and even a shift of the diurnal cycle with respect to the TSA region (see the contrary bias in the morning and afternoon). The daily amplitude, the difference between the maximum and minimum temperatures, is adequately represented in almost all simulations and regions, as the RDTR values for the months June/July in Fig. 10 demonstrate. The exception here is the EE region, with a daily cycle that is up to 20 percentage points too flat, whereas in the DUI region the daily amplitude is overestimated by up to 16 percentage points. In nearly all other cases, the positive and negative deviations of the daily temperature range are less than 10 percentage points.

https://doi.org/10.5194/egusphere-2026-1024
Preprint. Discussion started: 10 June 2026

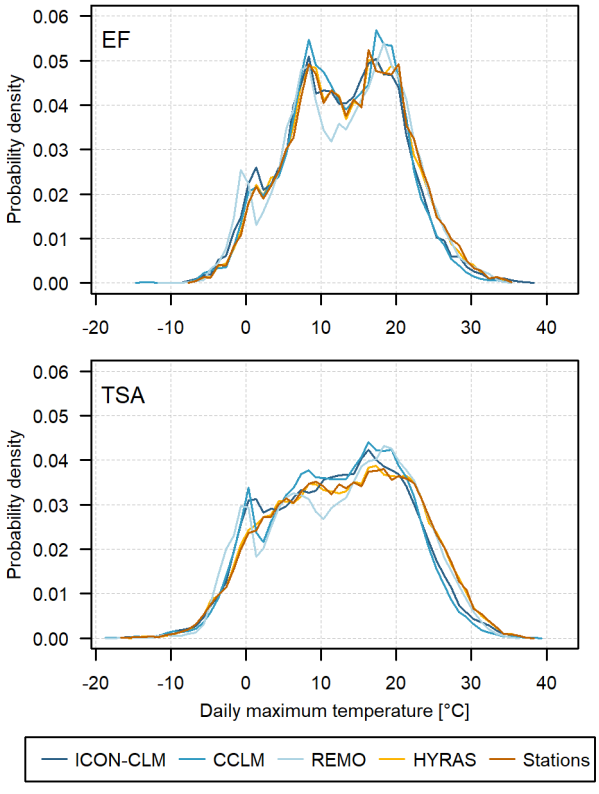

Figure 5. Frequency distribution of daily maximum temperature for the period 2005–2014 of the three CPM simulations on CEU-3 with ICON-CLM, CCLM, and REMO and the HYRAS reference data calculated over pilot regions EF (upper panel), and TSA (lower panel).

https://doi.org/10.5194/egusphere-2026-1024
Preprint. Discussion started: 10 June 2026

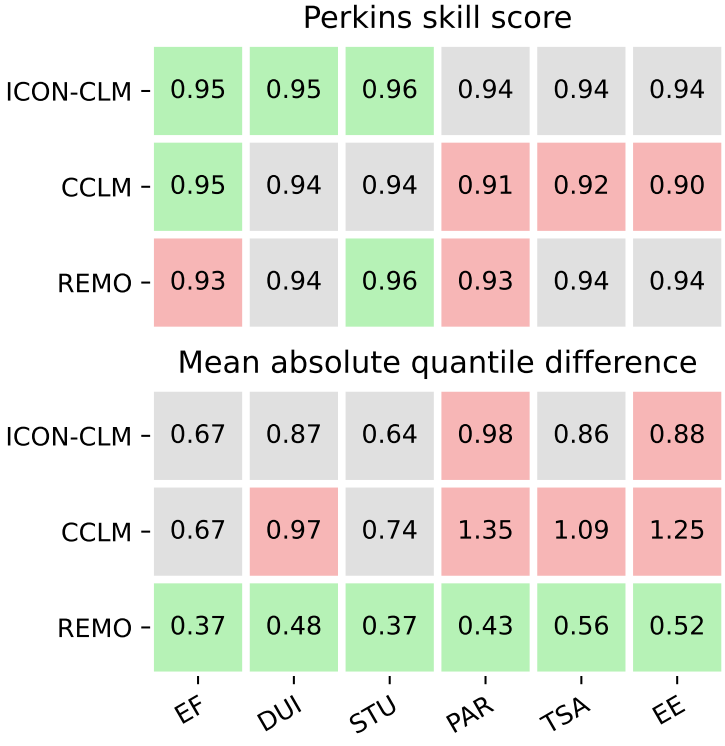

Figure 6. Perkins skill score (unit one) and mean absolute quantile difference (unit Kelvin) for daily maximum temperature with respect to HYRAS in all pilot regions and simulations. Meaning of coloured cells as in Fig. 4.

https://doi.org/10.5194/egusphere-2026-1024
Preprint. Discussion started: 10 June 2026

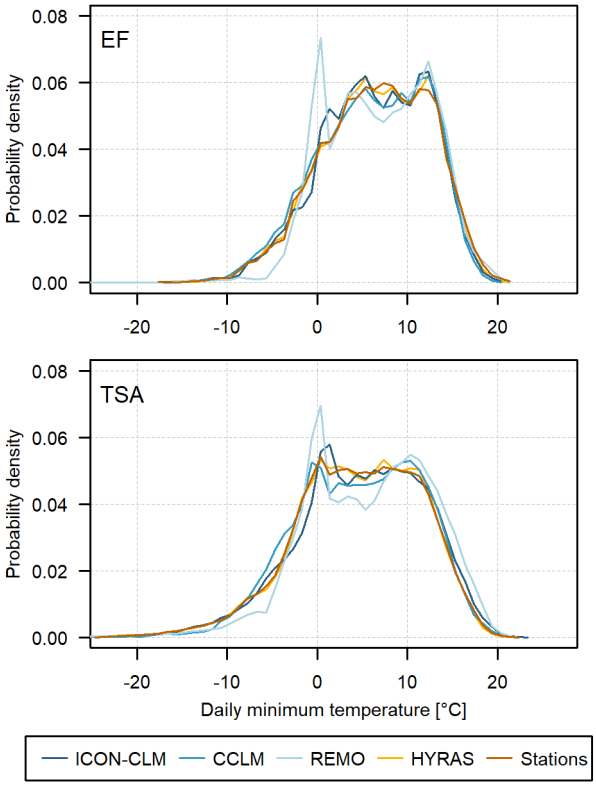

Figure 7. As Fig. 5 but for the daily minimum temperature.

https://doi.org/10.5194/egusphere-2026-1024
Preprint. Discussion started: 10 June 2026

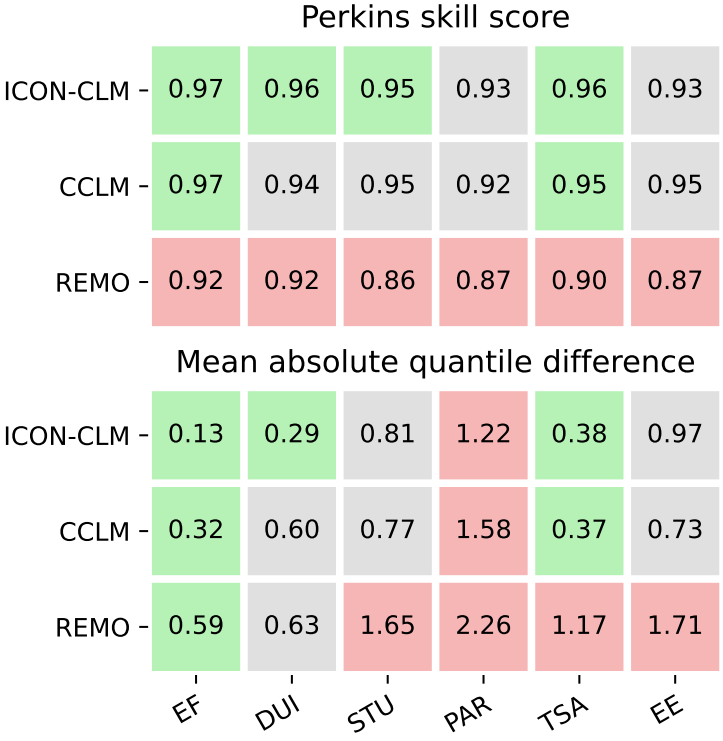

Figure 8. As Fig. 6 but for daily minimum temperature. Meaning of coloured cells as in Fig. 4.

https://doi.org/10.5194/egusphere-2026-1024
Preprint. Discussion started: 10 June 2026

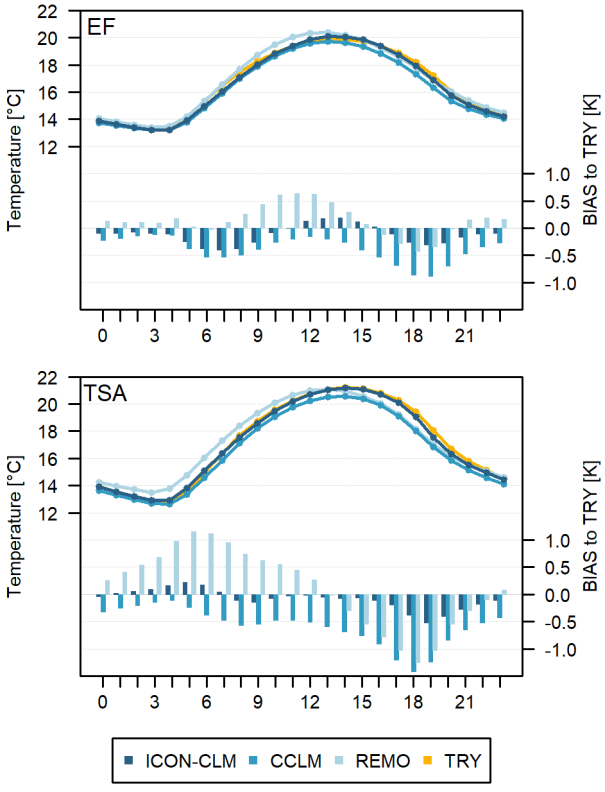

Figure 9. Diurnal cycle of 2 m temperature for the months June and July (curves, left axis) and temperature bias (shaded bars, right axis) for the period 2005–2014 and the three CPM simulations on CEU-3 with ICON-CLM (dark blue), CCLM (blue), and REMO (light blue) against TRY reference data (dark yellow curve) averaged over the pilot regions EF (upper panel) and TSA (lower panel).

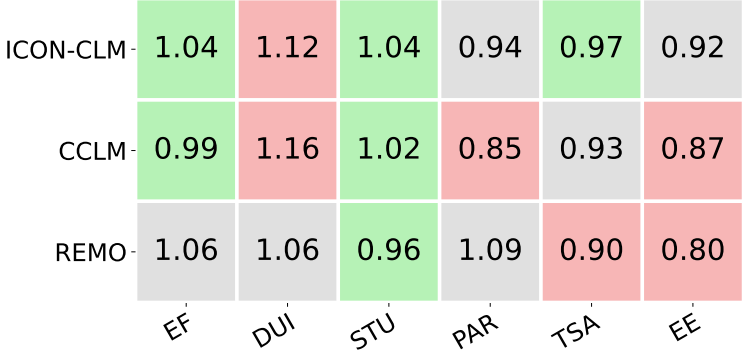

Figure 10. Ratio of the diurnal temperature range in 2 m height (unit one) for June and July of the period 2005–2014 with respect to TRY. The values are divided into three categories (terciles). Meaning of coloured cells as in Fig. 4.

https://doi.org/10.5194/egusphere-2026-1024
Preprint. Discussion started: 10 June 2026

3.2 Precipitation

The ICON-CLM simulation captures the mean annual precipitation very well. The relative deviations from the reference data in Fig. 11 are in the range of $\pm 10\,\%$ for large parts of Germany and nearly everywhere between $\pm 20\,\%$ with a tendency toward a higher relative bias in southern and eastern Germany.

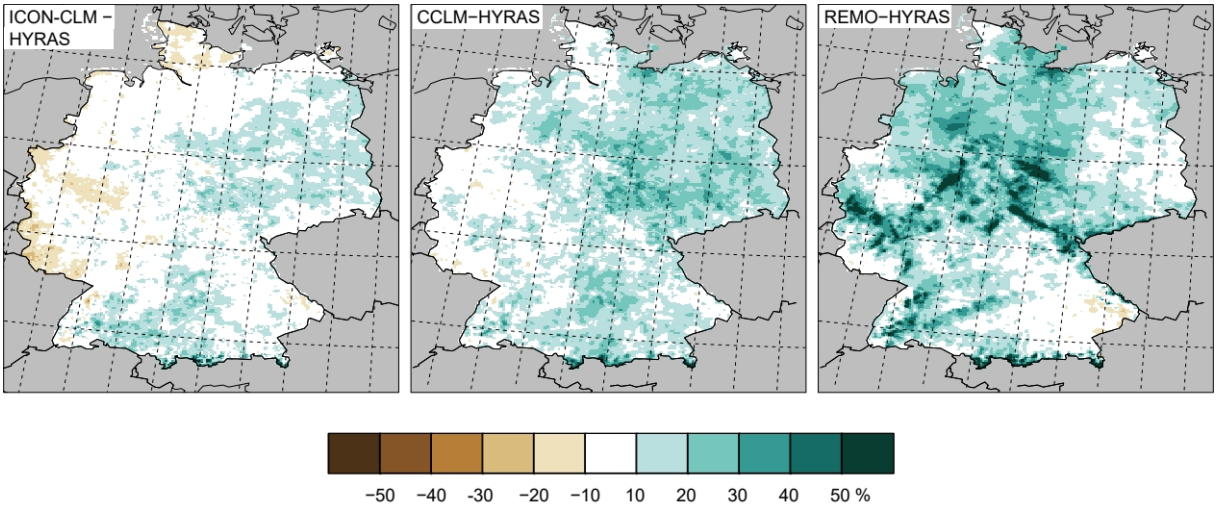

Figure 11. Relative mean annual precipitation bias for the period 2005–2014 on CEU-3 for the three CPM simulations with ICON-CLM, CCLM, and REMO from HYRAS reference data.

The CCLM simulation generally generates slightly more annual precipitation. However, the relative bias shows a spatial structure similar to that of the ICON-CLM simulation. The REMO simulation, on the other hand, shows a completely different structure of the annual precipitation bias. The relative deviations from the HYRAS data tend to be higher in northern Germany than in southern Germany and show singular hotspots along orographic structures with values greater than 50 %. This could be related to the different treatment of orography in REMO, which has not been smoothed with a spatial filter.

The simulated mean annual cycles of all models follow the temporal variation of the reference data in all pilot regions (Fig. 12 and Fig. S3) quite well. The monthly averages remain largely within the partly wide range of the station data. Compared to HYRAS, the simulations overestimate the annual amount of precipitation in all pilot regions, as the MB in Fig. 13 shows. The exception is the ICON-CLM simulation, which shows a slightly negative mean bias of 4 mm to 5 mm per month in the EE and DUI regions. The largest absolute deviations with values between 20 and 31 mm per month occur in all simulations in the PAR region. Here, almost all months show a pronounced positive bias, although in relative terms this is lowest in the summer months with a minimum in August (see Fig. S3 in the Supplementary Material) at absolutely higher monthly values. In all other regions and simulations, except CCLM and REMO in EF, the sign of the monthly deviations varies, with positive values dominating during the winter half-year.

https://doi.org/10.5194/egusphere-2026-1024
Preprint. Discussion started: 10 June 2026

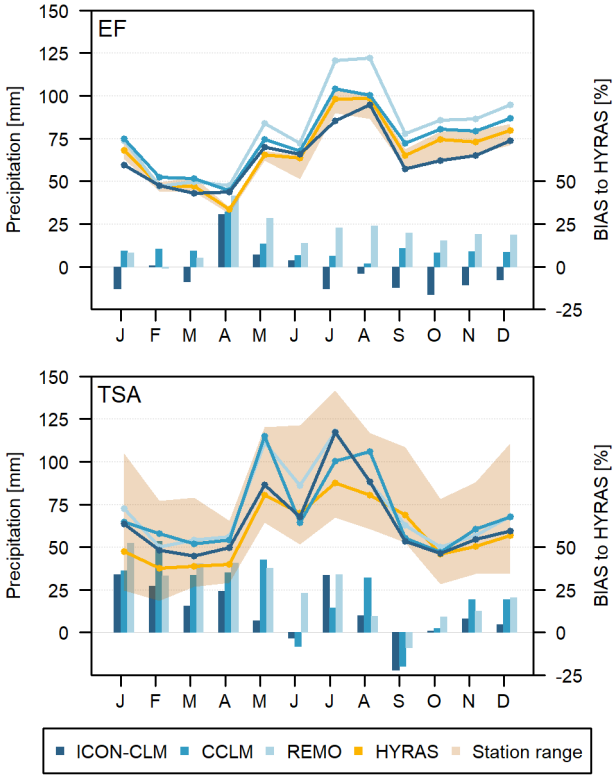

Figure 12. Annual cycle of mean monthly precipitation (curves, left axis) and precipitation bias (shaded bars, right axis) for the period 2005–2014 and the three CPM-simulations on CEU-3 with ICON-CLM (green), CCLM (blue) and REMO (red) against HYRAS reference data (dark yellow curve) averaged over the pilot regions EF (upper panel) and TSA (lower panel). The ochre-coloured range represent the span of corresponding values from observation stations located within the respective pilot region.

The general frequency distribution of precipitation amounts in Fig. 14 is well captured by all simulations and in all regions (see Fig. S11 in the Supplementary Material). This is documented by an excellent PSS in Fig. 15 of 0.96 or better for ICON-CLM and 0.94 or better for CCLM. The performance of the REMO simulation over the entire spectrum is poorer in all regions, especially in the pilot regions EF, DUI, TSA, and EE with PSS values not better than 0.85. At the high end of the distribution, extreme or very extreme precipitation with intensities of more than 20 mm or 40 mm per day generally occurs more frequently in the simulations than in the HYRAS data. The station data are usually closer to the HYRAS data than to the simulation data, with the exception of the EF region, but tend to have slightly higher probabilities than the HYRAS data for the extreme events. The better performance of the MAQD in the REMO simulation for the pilot regions STU, TSA, and EE results from lower frequencies of extreme precipitation events than in the ICON-CLM and the CCLM simulation and is therefore closer to the frequencies of the HYRAS data.

https://doi.org/10.5194/egusphere-2026-1024
Preprint. Discussion started: 10 June 2026

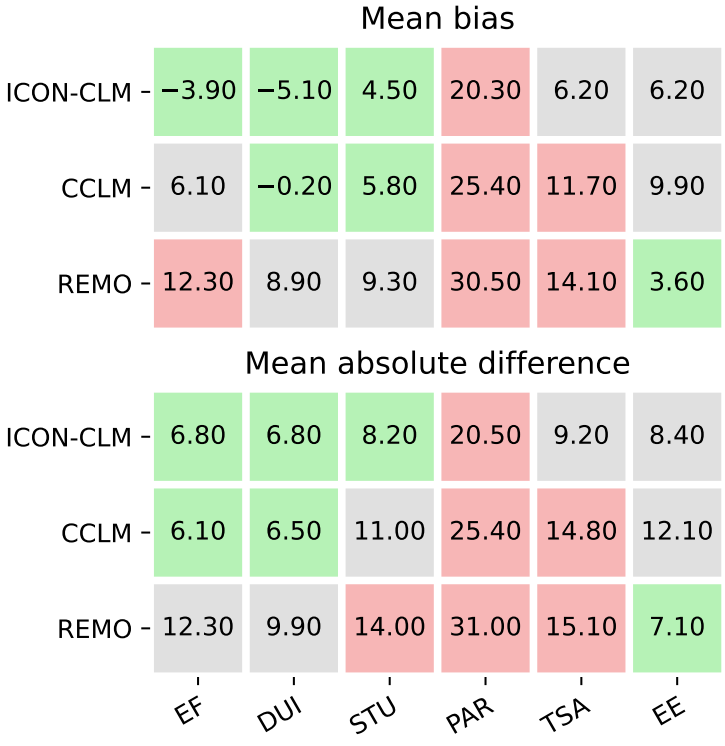

Figure 13. Mean bias and mean absolute difference of monthly precipitation in millimetres per month with respect to HYRAS for all pilot regions and simulations. Meaning of coloured cells as in Fig. 4.

Compared to other regions, for the coastal region EF the reference data exhibits a significantly dampened daily precipitation cycle (Fig. 16) due to less pronounced thermally-induced convection and the interaction with stably-stratified air over the North Sea. However, the models ICON-CLM and REMO show a more pronounced maximum in precipitation in the afternoon, whereas COSMO-CLM simulates a nocturnal peak.

The low mountain range region TSA has a different characteristic than EF, as it features a maximum in the late afternoon and another around midnight. The revival of precipitation at night could be due to convection triggered by the residual boundary layer and the air remaining warm in the evening (also characteristic for the region STU). While all models simulate an afternoon maximum in precipitation, the intensity and the timing varies a lot among the models. The second maximum at night does not appear in the simulations (except for ICON-CLM). In general, the models capture the daily cycle for TSA better than for EF as confirmed by the rank correlation coefficients (RCC) shown in Fig. 17. The RCC indicates poor performance particularly in regions that do not show a clear daily variation, as is also the case in the EE region (Fig. S6).

In regions with a clearly pronounced daily cycle, such as PAR (Fig. S6), the models do resolve an afternoon peak in precipitation, but amplitude and timing are not in line with the observations, leading to a slightly reduced RCC. Moreover, it can be observed that the morning convection minimum, seen in the observational data, is often captured.

https://doi.org/10.5194/egusphere-2026-1024
Preprint. Discussion started: 10 June 2026

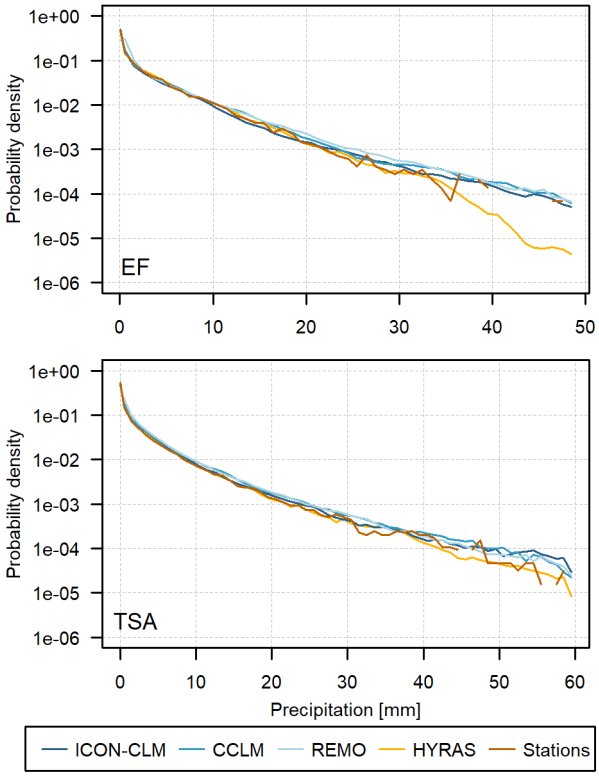

Figure 14. Frequency distribution of daily precipitation amounts for the period 2005–2014 of the three CPM simulations on CEU-3 with ICON-CLM, CCLM, and REMO, the HYRAS reference data, and mean station-based observations calculated over the pilot regions EF (upper panel) and TSA (lower panel).

It should be noted that REMO tends to overestimate the afternoon precipitation in many regions, even though this overestimation is less severe than shown in the graphs, because the precipitation amounts from the radar product used here tend to underestimate actual values (Kreklow et al., 2020). Since the deep convection parameterization is not active, deficiencies in cloud microphysics could be a plausible explanation.

https://doi.org/10.5194/egusphere-2026-1024
Preprint. Discussion started: 10 June 2026

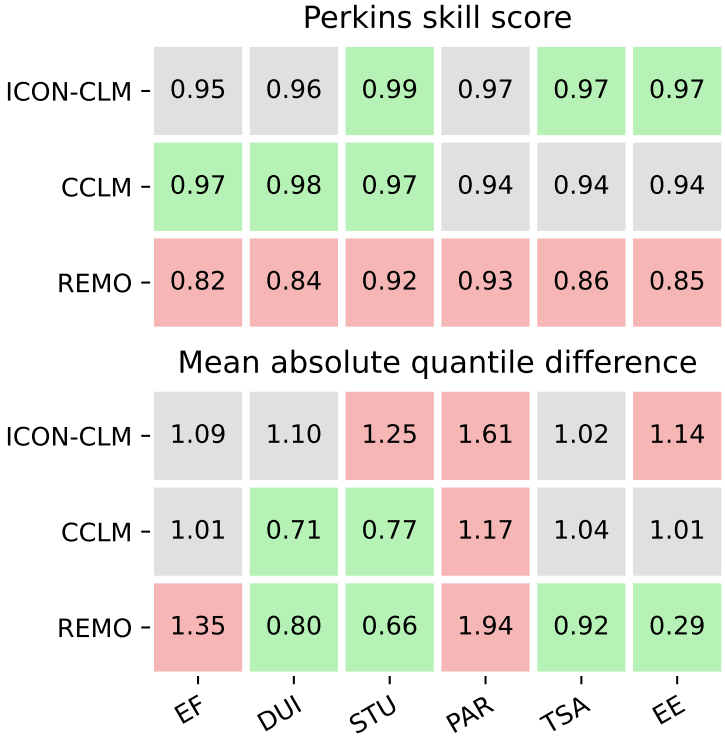

Figure 15. Perkins skill score (unit one) and mean absolute quantile difference (unit millimetre per day) for daily precipitation with respect to HYRAS. Meaning of coloured cells as in Fig. 4.

https://doi.org/10.5194/egusphere-2026-1024
Preprint. Discussion started: 10 June 2026

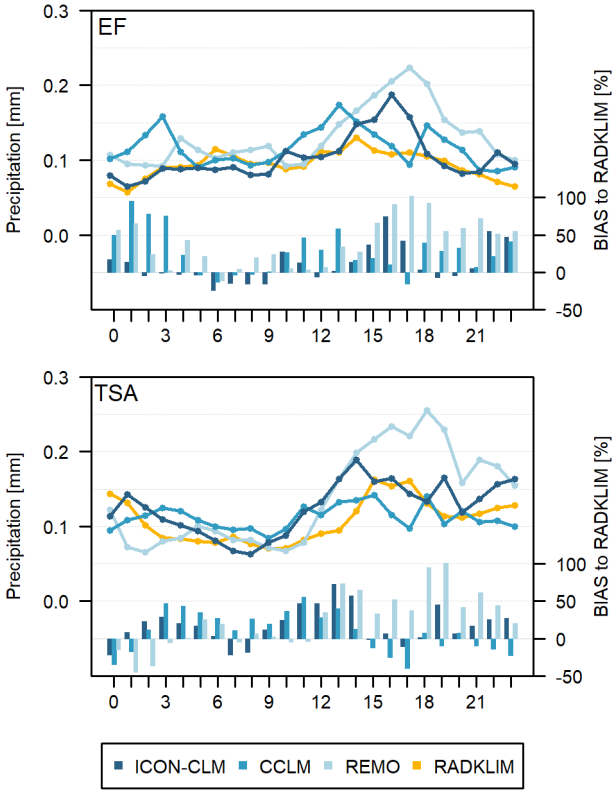

Figure 16. Diurnal cycle of precipitation for the months June and July (curves, left axis) and precipitation bias (shaded bars, right axis) for the period 2005–2014 and the three CP-simulations on CEU-3 with ICON-CLM (dark blue), CCLM (blue) and REMO (light blue) against RADKLIM v172 reference data (dark yellow curve) averaged over the pilot regions EF (upper panel) and TSA (lower panel).

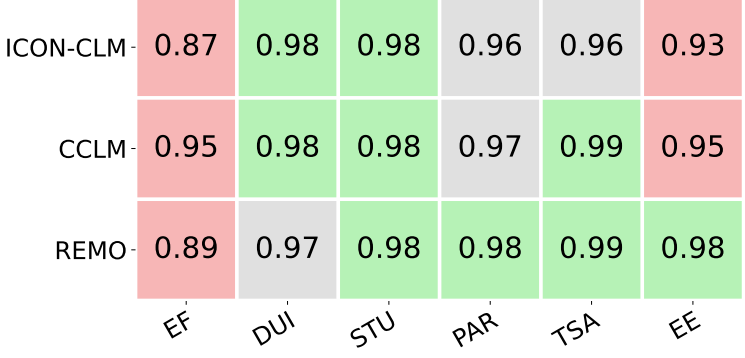

Figure 17. Rank Correlation Coefficient (unit 1) for the diurnal cycle of the precipitation with respect to RADKLIM averaged over the months June and July. Meaning of coloured cells as in Fig. 4.

https://doi.org/10.5194/egusphere-2026-1024
Preprint. Discussion started: 10 June 2026

3.3 Global Radiation

In general, the simulated diurnal cycle of global radiation is reasonable in all simulations (Fig. 18). Regarding the TSA region (and also the PAR region in S7), a small temporal shift and an overestimation of the peak radiation at noon (nearly 50 $\mathrm{W\,m^{-2}}$) are noticeable for the REMO model. Moreover, the radiation in the COSMO model is slightly underestimated during some morning hours (30 $\mathrm{W\,m^{-2}}$-40 $\mathrm{W\,m^{-2}}$). Regarding the EF region, the REMO simulation suffers from an underestimation of radiation in the afternoon, whereas the COSMO simulation suffers from an underestimation in the morning.

However, a comparison of hourly radiation has to be interpreted with care. The time of satellite retrieval and model output times are not the same because a shift of about 8 to 10 minutes is present for the SARAH product in the domain of Central Europe. Thus, a bias of less than 10 $\mathrm{W\,m^{-2}}$ can be the result of a sampling problem and not a model deficit. Moreover, different parameterizations of radiation were used in all three CPM simulations, which modify the cloudy-sky and clear-sky radiation. In addition, the representation of cloud cover is a key point for the simulation of radiation fluxes. In particular, the TSA region is affected by low mountain ranges with complex dynamics and cloud formation, which impedes its representation in atmospheric models.

The performance of the models for the diurnal cycle of radiation is quantified by the MAHD in Fig. 19 for all pilot regions. The relatively low values for ICON-CLM in all regions illustrate that the phase angle and amplitude of global radiation are best reproduced by this model. This is very likely due to the combination of using the sophisticated modern radiation scheme ecRad (Hogan and Bozzo, 2018) and an aerosol climatology, which best reflects the conditions of the simulated period. Compared to ICON-CLM, the COSMO-CLM offers slightly larger values for MAHD of about 3 $\mathrm{W\,m^{-2}}$ to 7 $\mathrm{W\,m^{-2}}$ larger. However, the REMO model reveals weak performance for the mountainous regions at STU, TSA and PAR. A possible reason might be too strong cloud developments because the daily cycle is overestimated a lot (see Fig. S6 in the Supplementary Material for precipitation cycles at PAR region).

https://doi.org/10.5194/egusphere-2026-1024
Preprint. Discussion started: 10 June 2026

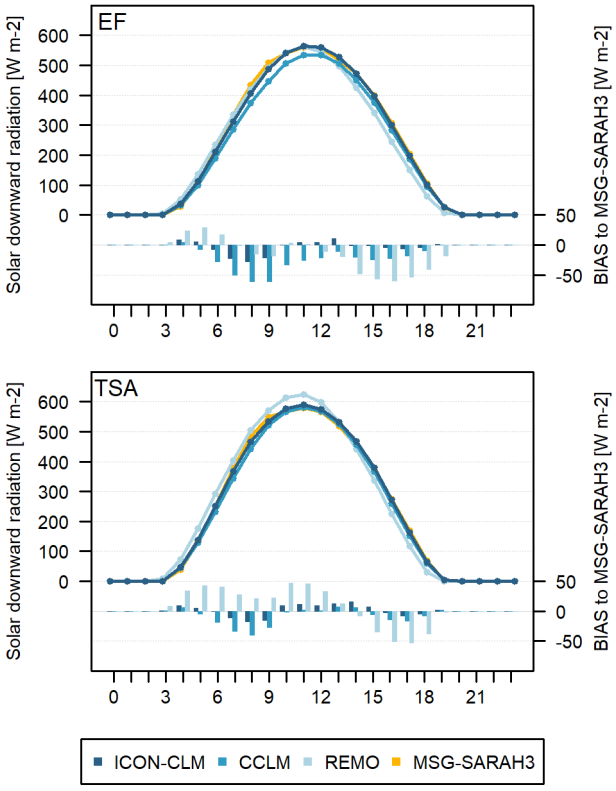

Figure 18. Diurnal cycle of solar downward radiation for the months June and July (curves, left axis) and radiation bias (shaded bars, right axis) for the period 2005–2014 and the three CPM simulations on CEU-3 with ICON-CLM (dark blue), CCLM (blue), and REMO (light blue) against MSG-SARAH3 reference data (dark yellow curve) averaged over the pilot regions EF (upper panel) and TSA (lower panel).

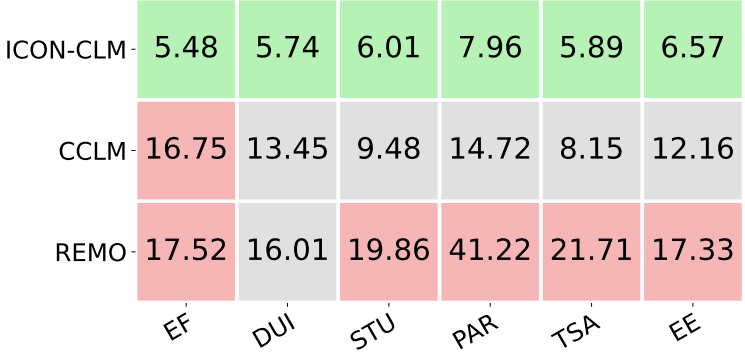

Figure 19. Mean absolute hourly differences (unit Watts per square meter) for global radiation with respect to MSG-SARAH3 averaged over the months June and July. Meaning of coloured cells as in Fig. 4.

https://doi.org/10.5194/egusphere-2026-1024
Preprint. Discussion started: 10 June 2026

3.4 10 m Wind Speed

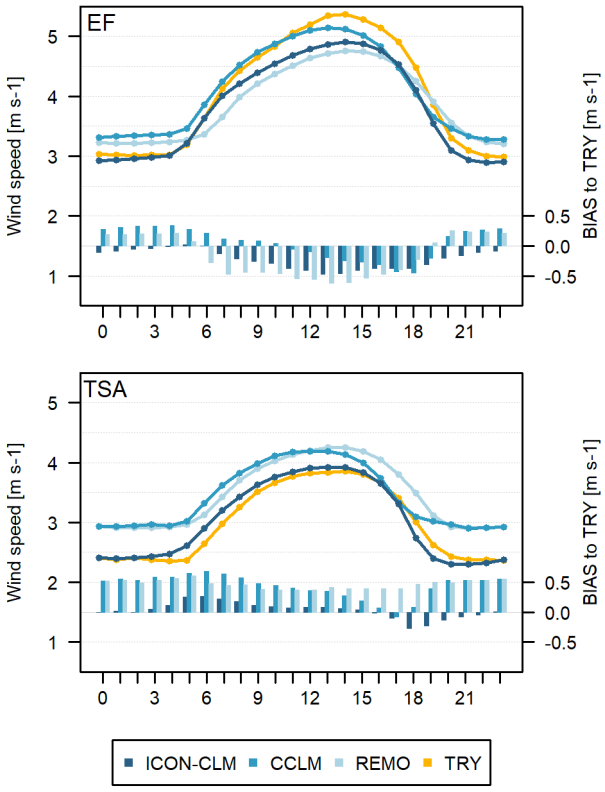

Figure 20. Diurnal cycle of 10 m wind speed for the months June and July (curves, left axis) and wind speed bias (shaded bars, right axis) for the period 2005–2014 and the three CPM simulations on CEU-3 with ICON-CLM (dark blue), CCLM (blue), and REMO (light blue) against TRY reference data (dark yellow curve) averaged over the pilot regions EF (upper panel) and TSA (lower panel).

Considering the evaluation of the mean diurnal cycle of the 10 m wind speed (Fig. 20), only ICON-CLM adequately represents the subsidence of wind at night during the summer season. REMO and COSMO-CLM overestimate the nighttime wind conditions by 0.5 $\mathrm{m\,s^{-1}}$. During the day, the incoming radiation triggers the development of a well-mixed planetary boundary layer with an increase in near-surface wind. This is well represented by all three models. However, the maximum peak in the afternoon and the amplitude of the daily cycle are underestimated in the EF region by all models. The REMO model underestimates the amplitude by about 0.8 $\mathrm{m\,s^{-1}}$. Moreover, the daily maximum value in COSMO-CLM and REMO suffers from a temporal shift of one hour. Remarkable is the connection between the model error and the transition from a nocturnal residual boundary layer to a well-mixed boundary layer during the day.

The greatest difficulties to reproduce the diurnal cycle of the 10 m wind speed during the summer months June and July occur in the pre Alpine region PAR resulting in a mean absolute hourly difference between 0.5 $\mathrm{m/s}$ and 0.9 $\mathrm{m/s}$ (Fig. 21).

https://doi.org/10.5194/egusphere-2026-1024
Preprint. Discussion started: 10 June 2026

All simulations underestimate here the wind speed substantially (Fig. S8) and show a stronger diurnal cycle than the observation based data set. One might get the impression that the circulation in mountainous regions as well as the land-sea breeze circulation, relevant for the EF region, is still challenging to be realistically simulated by the models. Despite the sometimes considerable deviations in intensity, the temporal progression of wind speed is reproduced very well by all models in all regions (with the exception of the PAR region). The quality is confirmed by small mean absolute hourly deviations from the reference data, mostly below 0.3 m in Fig. 21.

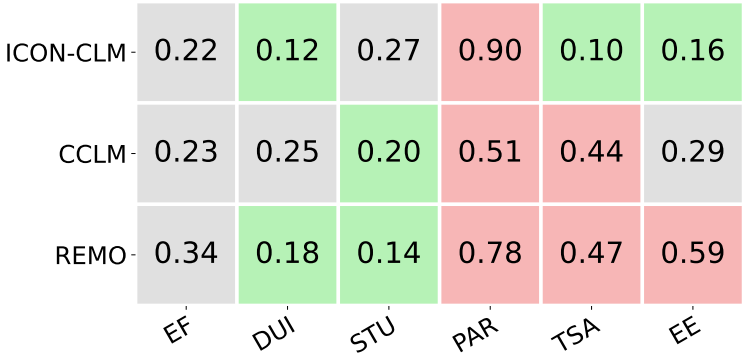

Figure 21. Mean absolute hourly difference for the diurnal cycle of the 10 m wind speed in metres per second with respect to TRY averaged over the months June and July. Meaning of coloured cells as in Fig. 4.

3.5 Climate Indices

Following the evaluation of the basic variables, we now evaluate the ensemble's ability to reproduce a selection of five climate indices: SU, HD, FD, R95ptot, and R20mm (Figure 22).

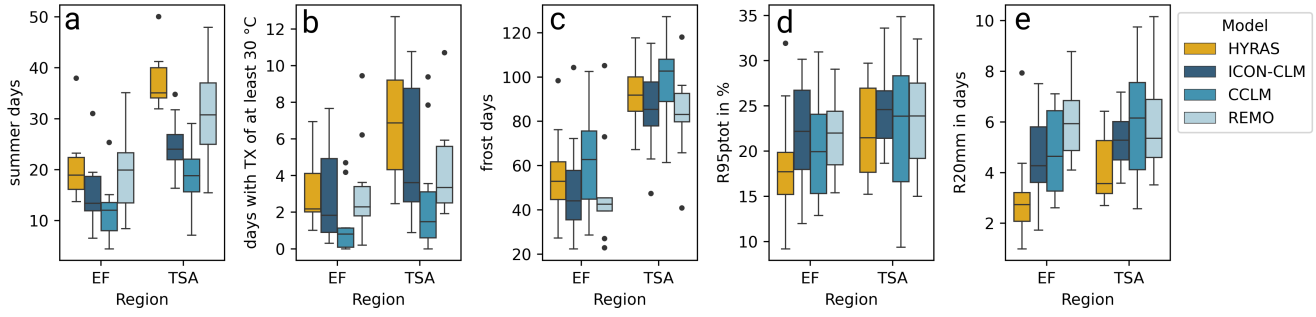

Figure 22. Distribution of the annual (a) Number of summer days (SU), (b) Number of hot days (HD), (c) Number of frost days (FD), (d) Contribution from very wet days (R95ptot), (e) Number of very heavy rain days (R20mm). The indices are averaged over the grid points in the respective pilot region.

https://doi.org/10.5194/egusphere-2026-1024
Preprint. Discussion started: 10 June 2026

The number of SU and HD is considerably larger in TSA compared to EF, a pattern reproduced by all ensemble members (Fig. 22 a and b). The underestimation of both climate indices by the models compared to HYRAS is consistent with a cold bias, especially for CCLM. This is consistent across all pilot regions (Fig. S4). The number of SU is also systematically underestimated in ICON-CLM, while REMO mostly covers the range of the observed number of summer days. However, it overestimates the inter-annual variability of SU, which is reflected in a wider spread of the distribution of SU in REMO. ICON-CLM and REMO also show the best representation of HD, particularly for the former. On the other hand, CCLM shows both low average values and low inter-annual variability. The maximum observed number of HD averaged over the region EF (DUI, STU) is exceeded in the ensemble. For the regions TSA (EE, PAR) the ensemble shows maximum values below the observation.

The number of FD are more frequent in the TSA region compared to the coastal region EF. The ensemble reproduces the number of FD within an absolute deviation of the median (maximum deviation of the single ensemble member's median from HYRAS) of 10 days in TSA, and 11 days in TSA. The ensemble covers the range of the observed number of FD for all assessed regions except the mountainous region PAR (Fig. S4). PAR has the highest number of FD and the ensemble shows a consistent underestimation. The result indicates a good agreement for regions with moderate temperatures, but a bias in cold regions. Within the ensemble, CCLM has the highest number of median FD for all regions. REMO tends to show the lowest median number of FD for EF, TSA, EE, STU, and PAR.

For the precipitation indices R95ptot and R20mm, HYRAS values for R95ptot are lower in EF than in TSA. This indicates that the proportion of precipitation from extreme events is greater in TSA than in the coastal region of EF. The same pattern is observed for the frequency of extreme precipitation (R20mm), which shows larger values for TSA. In both cases, the ensemble reproduces this regional pattern, albeit to a lesser extent for R20mm. For both EF and TSA, the ensemble shows a systematic overestimation of R95ptot. The smallest bias is found for the regions DUI and PAR (see Fig. S4). Also for the entire Germany domain the bias is small, indicating that the average behaviour is better represented in the ensemble due to a larger sample size or averaging of regional differences. The simulated spread compared to the observed spread, which is the inter-annual variability, is inconclusive. However, the analysis over the whole domain shows the lowest spread in the simulations. This may indicate that the ensemble does not represent the full range of inter-annual variability. R20mm is systematically overestimated in the simulations for most of the pilot regions (Fig. S4). The absolute bias is larger for regions with a high occurrence of R20mm events, and regional patterns seem to be preserved in the ensemble.

Overall, the evaluation of the climate indices indicates a systematic underestimation of heat stress and an apparent overestimation of frost days within the ensemble. The results for precipitation show on average a good representation of R95ptot and an overestimation of R20mm. The ensemble captures the maxima of the number of occurrences for the indices frost days, R20mm, R95ptot in single years. The observed years with maximum heat stress are not necessarily reproduced by the ensemble. We conclude that regional patterns in the different regions assessed are generally reproduced, but also document the need for bias correction as post-processing (Pinto et al., 2026).

https://doi.org/10.5194/egusphere-2026-1024
Preprint. Discussion started: 10 June 2026

4 Summary and Discussion

This study presents the evaluation of the first kilometre-scale, multi-model convection-permitting climate ensemble for Germany. Three regional climate models, ICON-CLM, COSMO-CLM, and REMO, were evaluated for the period 2005–2014 using a consistent modelling chain and a comprehensive set of reference datasets. The evaluation focused on fundamental meteorological variables (temperature, precipitation, radiation, wind), their diurnal and annual characteristics, and selected climate indices covering heat and precipitation extremes. Across variables and regions, the simulations demonstrate that convection-permitting modelling provides a substantial added value, capturing fine-scale structures and regional climatic features with good fidelity. However, each regional climate model exhibits characteristic strengths and weaknesses, and results document the need for bias correction where observational dates are available for calibration.

For temperature, all models reproduce the spatial temperature patterns and seasonal cycles well. ICON-CLM consistently shows the smallest biases, typically within $\pm 0.5\,\mathrm{K}$. COSMO-CLM exhibits a slight cold bias, while REMO tends toward warmer temperatures, particularly in southern Germany and the pre-alpine region. Compared to the CORDEX 12 km ensemble (Kotlarski et al., 2014), the NUKLEUS CPM ensemble exhibits lower biases and more realistic fine-scale structures, which confirms findings by Soares et al. (2024) or Hundhausen et al. (2023). Daily temperature distributions are well reproduced overall, although REMO shows broader distributions and less accurate minimum temperature extremes. Diurnal cycles are most realistically represented by ICON-CLM, while COSMO-CLM and REMO exhibit deviations in timing and amplitude.

Mean annual and monthly precipitation patterns are reasonably captured, but with model-specific deviations. ICON-CLM performs best overall, with moderate relative biases and a realistic annual cycle. COSMO-CLM exhibits a general overestimation, while REMO shows a distinctly different spatial bias structure, including local overestimation in northern Germany and along topographic structures. But in general the CPM simulations and specifically ICON-CLM improve the results compared to the old CORDEX ensemble (Kotlarski et al., 2014). Extreme precipitation frequencies are generally overestimated by all models, although REMO shows lower high-percentile occurrence than the other two RCMs with a good representation in the southeast of Germany. The overestimation of daily extremes is also confirmed in other studies on CPM simulations, (e.g., Lucas-Picher et al., 2021; Fowler et al., 2021; Hundhausen et al., 2024). Diurnal cycles reveal notable model deficiencies: afternoon peaks in the regions EF, TSA, and PAR are simulated too early or too intense, particularly with ICON-CLM and REMO. Ban et al. (2021) found similar results for a CPM ensemble over the Alps, however, compared to the convection parametrized coarser simulations they still found an improvement with respect to the representation of daily cycles.

All models reproduce the general shape of the diurnal radiation cycle, though with model- and region-specific amplitude biases. ICON-CLM performs best due to its modern radiation scheme. COSMO-CLM shows morning underestimation, while REMO shows over- or underestimation depending on region and cloud development. We are not aware of a comparable evaluation in the literature.

For wind, ICON-CLM is the only model able to realistically simulate the nocturnal wind minimum. COSMO-CLM and REMO tend to overestimate nighttime wind and show timing errors related to boundary-layer transitions. Up to now there are

https://doi.org/10.5194/egusphere-2026-1024
Preprint. Discussion started: 10 June 2026

few studies evaluating the wind speed in high resolution climate simulations. Molina et al. (2024) found some added value in CPM simulations compared to convection parametrized ensembles.

With climate indices, it was proven that the ensemble reproduces spatial patterns of heat and cold stress and precipitation extremes, though biases remain. Heat-related indices (Number of summer days and hot days) tend to be underestimated, especially for COSMO-CLM, reflecting its cold bias. Frost days are captured reasonably well, though are underestimated in colder high-elevation regions. Precipitation-based indices (precipitation on very wet days and number of very heavy rain days) are systematically overestimated, but regional contrasts as, e.g., higher extremes in mountainous regions are preserved. These results are promising regarding the use of climate model driven simulations to quantify the impact of climate change for different stakeholders and sectors (Buontempo et al., 2018; Pinto et al., 2026), which will the focus of two separate manuscripts.

The NUKLEUS CPM ensemble provides a substantial advancement in high-resolution climate information for Germany, offering improved representation of convective processes, regional climate features, and local extremes compared to coarser regional or global models. Despite this progress, the evaluation highlights model-specific systematic biases, especially regarding extreme precipitation, diurnal cycle behaviour, and temperature extremes in complex terrain. These findings underpin the importance of multi-model ensembles for robust regional climate assessment and highlight areas for further development, including improved cloud microphysics, boundary-layer representation, and radiation schemes. Overall, the ensemble demonstrates strong potential as a foundation for actionable climate information, especially in the context of regional climate adaptation efforts within the RegIKlim program. To address this main aim of the RegIKlim program, the used RCMs, their setups, and the domains described in this study are applied to create the final NUKLEUS ensemble of CPM climate simulations for the historical reference period and two future periods representing two different states of global warming. These simulations will be introduced and evaluated in two follow-up studies (Braun et al., 2026; Beier et al., 2026). Furthermore, a study focusing on the added-value of the 3 km CEU-3 simulations compared to the 12 km EUR-11 simulations of the final NUKLEUS ensemble is in preparation (Baumann and Paeth, 2026).

Code and data availability. The ICON release icon-2.6.6 was used for the for the ICON simulations. Only more recent versions are published under open access (e.g., https://doi.org/10.35089/WDCC/IconRelease2024.07, ICON 2024). Results can be reproduced with the later model version within the range of model intrinsic variability. The used model version can made available on demand. The execution of the job workflow for ICON was managed using SPICE - Starter Package for ICON-CLM Experiments, specifically the version 2.1 released in January 2022 (https://zenodo.org/records/6838984, Rockel and Geyer, 2022b), which is publicly available on Zenodo. The final release of COSMO (cosmo6.0) was applied. The documentation of the COSMO model is developed by the COSMO Consortium and consists of user guide and scientific documentation. It is permanently available at: https://www.dwd.de/EN/ourservices/cosmo_documentation/cosmo_documentation.html (last access: 12 January 2026). The COSMO-CLM model is free of charge for all research applications; however, access is license-restricted: https://www.cosmo-model.org/content/consortium/licencing.htm (last access: 12 January 2026). To download, the user needs to become a member of the CLM-Community or the respective institute needs to hold an institutional license. The execution of the job workflow for COSMO was managed using the Starter Package for COSMO-CLM Experiments, specifically the version 5.0 released in February 2022 (https://doi.org/10.5281/zenodo.7290478, Rockel and Geyer, 2022a), which is publicly available on Zenodo. The sources for

https://doi.org/10.5194/egusphere-2026-1024
Preprint. Discussion started: 10 June 2026

the REMO model are available on request from the Climate Service Center Germany (contact@remo-rcm.de). Open access is not possible due to licensing limitations coming from the legacy code within REMO. The version used in this work is saved and archived on Zenodo (https://doi.org/10.5281/zenodo.15679389). NUKLEUS data available at the German Climate Computing Centre (DKRZ); requires login: https://www-regiklim.dkrz.de/. Further information on the available data can be found at: https://ch1187.gitlab-pages.dkrz.de/Information/Data.html. An openly available access is planned for September 2026 in a data portal at DKRZ that is part of the funding of the NUKLEUS project and currently under development.

Author contributions. The conceptualisation and methodology was developed by KK, RP, HF, KS and JGP. The model development was done by RP, KK, BG, HF, KS, TF. The simulations were conducted by RP, BG, TF, HF, KK. Plotting routines and figure production were done by RP, CBe, MH and BG. The preparation of the external data was done by RP, KK, TF. The result analysis and discussion and proof reading were done by all co-authors. The paper writing was done by KS, JGP, KK, CBe, HF, BG, RP, MH with contributions from CB, PH, and FE. Overall management of the collaboration was done by KS and JGP.

Competing interests. The authors declare that they have no conflict of interest.

Acknowledgements. This study was funded by the German Federal Ministry of Research, Technology and Space (BMFTR) project RegIKlim-NUKLEUS (01LR2002A-G, 01LR2002A1-G1). MH was funded by RegIKlim-ISAP (01LR2007B, 01LR2007B1) for support. HF and JGP received funding from the BMFTR project ClimXtreme (01LP1901A, 01LP2322A). JGP thanks the AXA Research Fund for support. We acknowledge the DKRZ for the use of resources in terms of granted computing time and storage capacity (projects bg1187 and bb1203). Additionally, we used data from the DKRZ /pool/data section provided by the CLM Community. We further thank Deutscher Wetterdienst (DWD) for providing the HYRAS, TRY, and RADKLIM data sets as well as the German station data. We thank Michael Woldt (BTU Cottbus-Senftenberg) who supported the ICON-CLM simulations and data postprocessing.

https://doi.org/10.5194/egusphere-2026-1024
Preprint. Discussion started: 10 June 2026

References

Alexander, L. and Herold, N.: ClimPACT2: Indices and software, https://hdl.handle.net/10013/epic.94f52968-eeed-4766-9285-5c3466c98932, 2016.

Baldauf, M.: A new fast-waves solver for the Runge-Kutta dynamical core, Tech. Rep. 21, Deutscher Wetterdienst, https://doi.org/10.5676/DWD_pub/nwv/cosmo-tr_21, 2013.

Baldauf, M., Seifert, A., Förstner, J., Majewski, D., Raschendorfer, M., and Reinhardt, T.: Operational Convective-Scale Numerical Weather Prediction with the COSMO Model: Description and Sensitivities, Monthly Weather Review, 139, 3887–3905, https://doi.org/10.1175/MWR-D-10-05013.1, 2011.

Ban, N., Caillaud, C., Coppola, E., Pichelli, E., Sobolowski, S., Adinolfi, M., Ahrens, B., Alias, A., Anders, I., Bastin, S., Belušić, D., Berthou, S., Brisson, E., Cardoso, R. M., Chan, S. C., Christensen, O. B., Fernández, J., Fita, L., Frisius, T., Gašparac, G., Giorgi, F., Goergen, K., Haugen, J. E., Hodnebrog, Ø., Kartsios, S., Katragkou, E., Kendon, E. J., Keuler, K., Lavin-Gullon, A., Lenderink, G., Leutwyler, D., Lorenz, T., Maraun, D., Mercogliano, P., Milovac, J., Panitz, H.-J., Raffa, M., Remedio, A. R., Schär, C., Soares, P. M. M., Srnec, L., Steensen, B. M., Stocchi, P., Tölle, M. H., Truhetz, H., Vergara-Temprado, J., de Vries, H., Warrach-Sagi, K., Wulfmeyer, V., and Zander, M. J.: The first multi-model ensemble of regional climate simulations at kilometer-scale resolution, part I: evaluation of precipitation, Climate Dynamics, 57, 275–302, https://doi.org/10.1007/s00382-021-05708-w, 2021.

Baumann, M. and Paeth, H.: NUKLEUS – A First Kilometre-Scale Multi-model Climate Ensemble for Germany: Added Value of Convection-Permitting Simulations for Variability, Extremes, and Trends under Bias Correction, Info, in preparation, 2026.

Bechtold, P., Koehler, M., Jung, T., Doblas-Reyes, F., Leutbecher, M., Rodwell, M. J., Vitart, F., and Balsamo, G.: Advances in simulating atmospheric variability with the ECMWF model: From synoptic to decadal time-scales, Quarterly Journal of the Royal Meteorological Society, 134, 1337–1351, https://doi.org/10.1002/qj.289, 2008.

Beier, C., Ziegler, K., Paeth, H., Pinto, J. G., Sieck, K., Buntemeyer, L., Geyer, B., Xoplaki, E., Espitia, E., Braun, C., Ehmele, F., Feldmann, H., Kadow, C., and Trachte, K.: NUKLEUS - A First Convection Permitting Multi-model Ensemble for Germany: Assessment of future changes in temperature and precipitation extremes, Journal of Climate, in preparation, 2026.

Berthou, S., Kendon, E. J., Chan, S. C., Ban, N., Leutwyler, D., Schär, C., and Fosser, G.: Pan-European climate at convection-permitting scale: a model intercomparison study, Climate Dynamics, 55, 35–59, https://doi.org/10.1007/s00382-018-4114-6, 2020.

Braun, C., Ehmele, F., Beier, C., Espitia-Sarmiento, E. F., Feldmann, H., Frisius, T., Geyer, B., Hundhausen, M., Keuler, K., Luterbacher, J., Sieck, K., Trachte, K., Xoplaki, E., and Pinto, J. G.: NUKLEUS - A first kilometer-scale convection-permitting multi-model climate ensemble for Germany: Characteristics of the historical simulations, Geoscientific Model Development, submitted, 2026.

Buontempo, C., Hanlon, H. M., Bruno Soares, M., Christel, I., Soubeyroux, J.-M., Viel, C., Calmanti, S., Bosi, L., Falloon, P., Palin, E. J., Vanvyve, E., Torralba, V., Gonzalez-Reviriego, N., Doblas-Reyes, F., Pope, E. C., Newton, P., and Liggins, F.: What have we learnt from EUPORIAS climate service prototypes?, Climate Services, 9, 21–32, https://doi.org/10.1016/j.cliser.2017.06.003, 2018.

Commission, E., for Research, D.-G., and Innovation: EU Missions : adaptation to climate change : concrete solutions for our greatest challenges, Publications Office of the European Union, https://doi.org/doi/10.2777/88566, 2021.

Coppola, E., Sobolowski, S., Pichelli, E., Raffaele, F., Ahrens, B., Anders, I., Ban, N., Bastin, S., Belda, M., Belusic, D., Caldas-Alvarez, A., Cardoso, R. M., Davolio, S., Dobler, A., Fernandez, J., Fita, L., Fumiere, Q., Giorgi, F., Goergen, K., Güttler, I., Halenka, T., Heinzeller, D., Hodnebrog, Ø., Jacob, D., Kartsios, S., Katragkou, E., Kendon, E., Khodayar, S., Kunstmann, H., Knist, S., Lavín-Gullón, A., Lind, P., Lorenz, T., Maraun, D., Marelle, L., van Meijgaard, E., Milovac, J., Myhre, G., Panitz, H.-J., Piazza, M., Raffa, M., Raub, T., Rockel,

https://doi.org/10.5194/egusphere-2026-1024
Preprint. Discussion started: 10 June 2026

B., Schär, C., Sieck, K., Soares, P. M. M., Somot, S., Srnec, L., Stocchi, P., Tölle, M. H., Truhetz, H., Vautard, R., de Vries, H., and Warrach-Sagi, K.: A first-of-its-kind multi-model convection permitting ensemble for investigating convective phenomena over Europe and the Mediterranean, Climate Dynamics, 55, 3–34, https://doi.org/10.1007/s00382-018-4521-8, 2018.

Davies, H. C.: A lateral boundary formulation for multi-level prediction models, Quarterly Journal of the Royal Meteorological Society, 102, 405–418, https://doi.org/10.1002/qj.49710243210, 1976.

Dee, D. P., Uppala, S. M., Simmons, A. J., Berrisford, P., Poli, P., Kobayashi, S., Andrae, U., Balmaseda, M. A., Balsamo, G., Bauer, P., Bechtold, P., Beljaars, A. C. M., van de Berg, L., Bidlot, J., Bormann, N., Delsol, C., Dragani, R., Fuentes, M., Geer, A. J., Haimberger, L., Healy, S. B., Hersbach, H., Hólm, E. V., Isaksen, L., Kållberg, P., Köhler, M., Matricardi, M., McNally, A. P., Monge-Sanz, B. M., Morcrette, J.-J., Park, B.-K., Peubey, C., de Rosnay, P., Tavolato, C., Thépaut, J.-N., and Vitart, F.: The ERA-Interim Reanalysis: Configuration and Performance of the Data Assimilation System, Quarterly Journal of the Royal Meteorological Society, 137, 553–597, https://doi.org/10.1002/qj.828, 2011.

Doms, G., Foerstner, J., Heise, E., Herzog, H.-J., Mironov, D., Raschendorfer, M., Reinhardt, T., Ritter, B., Schrodin, R., Schulz, J.-P., and Gerd, V.: A Description of the Nonhydrostatic Regional COSMO-Model. Part II Physical Parameterizations, Tech. rep., Deutscher Wetterdienst, https://doi.org/10.5676/DWD_pub/nwv/cosmo-doc_6.00_II, 2021.

Doury, A., Somot, S., Gadat, S., Ribes, A., and Corre, L.: Regional climate model emulator based on deep learning: concept and first evaluation of a novel hybrid downscaling approach, Climate Dynamics, 60, 1751–1779, https://doi.org/10.1007/s00382-022-06343-9, 2023.

ETCCDI: Expert Team on Climate Change Detection and Indices, https://www.clivar.org/organization/etccdi/etccdi.php, 2014.

EUCP Project Team: EUCP convection-permitting model simulations. EUCP Data Catalogue., https://eucp-project.github.io/data-catalogue/cpm/, 2021.

Eyring, V., Gillett, N. P., Achuta Rao, K. M., Barimalala, R., Barreiro Parrillo, M., Bellouin, N., Cassou, C., Durack, P. J., Kosaka, Y., McGregor, S., Min, S.-K., Morgenstern, O., and Sun, Y.: Human Influence on the Climate System, in: Climate Change 2021: The Physical Science Basis. Contribution of Working Group I to the Sixth Assessment Report of the Intergovernmental Panel on Climate Change, edited by Masson-Delmotte, V., Zhai, P., Pirani, A., Connors, S. L., Péan, C., Berger, S., Caud, N., Chen, Y., Goldfarb, L., Gomis, M. I., Huang, M., Leitzell, K., Lonnoy, E., Matthews, J. B. R., Maycock, T. K., Waterfield, T., Yelekçi, O., Yu, R., and Zhou, B., pp. 423–552, Cambridge University Press, Cambridge, United Kingdom and New York, NY, USA, https://doi.org/10.1017/9781009157896.005, 2021.

Fowler, H. J., Ali, H., Allan, R. P., Ban, N., Barbero, R., Berg, P., Blenkinsop, S., Cabi, N. S., Chan, S., Dale, M., Dunn, R. J. H., Ekström, M., Evans, J. P., Fosser, G., Golding, B., Guerreiro, S. B., Hegerl, G. C., Kahraman, A., Kendon, E. J., Lenderink, G., Lewis, E., Li, X., O'Gorman, P. A., Orr, H. G., Peat, K. L., Prein, A. F., Pritchard, D., Schär, C., Sharma, A., Stott, P. A., Villalobos-Herrera, R., Villarini, G., Wasko, C., Wehner, M. F., Westra, S., and Whitford, A.: Towards advancing scientific knowledge of climate change impacts on short-duration rainfall extremes, Philosophical Transactions of the Royal Society A: Mathematical, Physical and Engineering Sciences, 379, 20190 542, https://doi.org/10.1098/rsta.2019.0542, 2021.

Fünfgeld, H., Fila, D., and Dahlmann, H.: Upscaling climate change adaptation in small- and medium-sized municipalities: current barriers and future potentials, Current Opinion in Environmental Sustainability, 61, 101 263, https://doi.org/10.1016/j.cosust.2023.101263, 2023.

Fünfgeld, H., Christen, A., Briegel, F., Schrodi, S., Speidel, A., Felder, C., Hoffmann, J., Irscheid, L., Merkle, D., Meyer, J., Schindler, D., Wehrle, J., and Zengerling, C.: Optimizing urban greening and densification in the context of outdoor heat: Opportunities for AI-supported urban adaptation, Landscape and Urban Planning, 268, 105 574, https://doi.org/10.1016/j.landurbplan.2025.105574, 2026.

https://doi.org/10.5194/egusphere-2026-1024
Preprint. Discussion started: 10 June 2026

Giorgetta, M. A., Brokopf, R., Crueger, T., Esch, M., Fiedler, S., Helmert, J., Hohenegger, C., Kornblueh, L., Koehler, M., Manzini, E., Mauritsen, T., Nam, C., Raddatz, T., Rast, S., Reinert, D., Sakradzija, M., Schmidt, H., Schneck, R., Schnur, R., Silvers, L., Wan, H., Zaengl, G., and Stevens, B.: ICON-A, the Atmosphere Component of the ICON Earth System Model: I. Model Description, Journal of Advances in Modeling Earth Systems, 10, 1613–1637, https://doi.org/10.1029/2017MS001242, 2018.

Giorgi, F., Jones, C., and Asrar, G.: Addressing climate information needs at the regional level: The CORDEX framework, WMO Bull, 53, 175–183, 2009.

Göttel, H.: Einfluss der nichthydrostatischen Modellierung und der Niederschlagsverdriftung auf die Ergebnisse regionaler Klimamodellierung, Ph.D. thesis, Max-Planck-Institut für Meteorologie, https://doi.org/10.17617/2.994076, 2009.

Gutiérrez, J. M., Maraun, D., Widmann, M., Huth, R., Hertig, E., Benestad, R., Roessler, O., Wibig, J., Wilcke, R., Kotlarski, S., San Martín, D., Herrera, S., Bedia, J., Casanueva, A., Manzanas, R., Iturbide, M., Vrac, M., Dubrovsky, M., Ribalaygua, J., Pórtoles, J., Räty, O., Räisänen, J., Hingray, B., Raynaud, D., Casado, M. J., Ramos, P., Zerenner, T., Turco, M., Bosshard, T., Štěpánek, P., Bartholy, J., Pongracz, R., Keller, D. E., Fischer, A. M., Cardoso, R. M., Soares, P. M. M., Czernecki, B., and Pagé, C.: An intercomparison of a large ensemble of statistical downscaling methods over Europe: Results from the VALUE perfect predictor cross-validation experiment, International Journal of Climatology, 39, 3750–3785, https://doi.org/10.1002/joc.5462, 2019.

Gutowski Jr., W. J., Giorgi, F., Timbal, B., Frigon, A., Jacob, D., Kang, H.-S., Raghavan, K.and Lee, B., Lennard, C., Nikulin, G., O'Rourke, E., Rixen, M.and Solman, S., Stephenson, T., and Tangang, F.: WCRP COordinated Regional Downscaling EXperiment (CORDEX): a diagnostic MIP for CMIP6, Geoscientific Model Development, 9, 4087–4095, https://doi.org/10.5194/gmd-9-4087-2016, 2016.

Hammoudeh, S., Goergen, K., Belleflamme, A., Giles, J. A., Troemel, S., and Kollet, S.: Evaluating precipitation products for water resources hydrologic modeling over Germany, Frontiers in Earth Science, 13, 1548 557, https://doi.org/10.3389/feart.2025.1548557, 2025.

Hänsler, A. and Weiler, M.: Enhancing the usability of weather radar data for the statistical analysis of extreme precipitation events, Hydrology and Earth System Sciences, 26, 5069–5084, https://doi.org/10.5194/hess-26-5069-2022, 2022.

Heinze, R., Dipankar, A., Henken, C. C., Moseley, C., Sourdeval, O., Troemel, S., Xie, X., Adamidis, P., Ament, F., Baars, H., Barthlott, C., Behrendt, A., Blahak, U., Bley, S., Brdar, S., Brueck, M., Crewell, S., Deneke, H., Di Girolamo, P., Evaristo, R., Fischer, J., Frank, C., Friederichs, P., Goecke, T., Gorges, K., Hande, L., Hanke, M., Hansen, A., Hege, H.-C., Hoose, C., Jahns, T., Kalthoff, N., Klocke, D., Kneifel, S., Knippertz, P., Kuhn, A., van Laar, T., Macke, A., Maurer, V., Mayer, B., Meyer, C. I., Muppa, S. K., Neggers, R. A. J., Orlandi, E., Pantillon, F., Pospichal, B., Roeber, N., Scheck, L., Seifert, A., Seifert, P., Senf, F., Siligam, P., Simmer, C., Steinke, S., Stevens, B., Wapler, K., Weniger, M., Wulfmeyer, V., Zaengl, G., Zhang, D., and Quaas, J.: Large-eddy simulations over Germany using ICON: a comprehensive evaluation, Quarterly Journal of the Royal Meteorological Society, 143, 69–100, https://doi.org/10.1002/qj.2947, 2017.

Hersbach, H., Bell, B., Berrisford, P., Hirahara, S., Horányi, A., Muñoz-Sabater, J., Nicolas, J., Peubey, C., Radu, R., Schepers, D., Simmons, A., Soci, C., Abdalla, S., Abellan, X., Balsamo, G., Bechtold, P., Biavati, G., Bidlot, J., Bonavita, M., De, Giovanna, D., Dahlgren, P., Dee, D., Diamantakis, M., Dragani, R., Flemming, J., Forbes, R., Fuentes, M., Geer, A., Haimberger, L., Healy, S., J., Robin, J., Hólm, E., Janisková, M., Keeley, S., Laloyaux, P., Lopez, P., Lupu, C., Radnoti, G., de, Patricia, d., Rozum, I., Vamborg, F., Villaume, S., and Thépaut, J.-N.: The ERA5 global reanalysis, Quarterly Journal of the Royal Meteorological Society, 146, 1999–2049, https://doi.org/10.1002/qj.3803, 2020.

Hewitt, C. D. and Lowe, J. A.: Toward a European Climate Prediction System, Bulletin of the American Meteorological Society, 99, 1997–2001, https://doi.org/10.1175/BAMS-D-18-0022.1, 2018.

Hogan, R. J. and Bozzo, A.: A Flexible and Efficient Radiation Scheme for the ECMWF Model, Journal of Advances in Modeling Earth Systems, 10, 1990–2008, https://doi.org/10.1029/2018MS001364, 2018.

https://doi.org/10.5194/egusphere-2026-1024
Preprint. Discussion started: 10 June 2026

Hundhausen, M., Feldmann, H., Laube, N., and Pinto, J. G.: Future heat extremes and impacts in a convection-permitting climate ensemble over Germany, Natural Hazards and Earth System Sciences, 23, 2873–2893, https://doi.org/10.5194/nhess-23-2873-2023, 2023.

Hundhausen, M., Feldmann, H., Kohlhepp, R., and Pinto, J. G.: Climate change signals of extreme precipitation return levels for Germany in a transient convection-permitting simulation ensemble, International Journal of Climatology, 44, 1454–1471, https://doi.org/10.1002/joc.8393, 2024.

Hundhausen, M., Fowler, H. J., Feldmann, H., and Pinto, J. G.: Sub-hourly precipitation and rainstorm event profiles in a convection-permitting multi-GCM ensemble, Weather and Climate Extremes, 48, 100 764, https://doi.org/10.1016/j.wace.2025.100764, 2025.

ICON partnership (DWD and MPI-M and DKRZ and KIT and C2SM): ICON release 2024.07, https://doi.org/10.35089/WDCC/IconRelease2024.07, 2024.

Jacob, D. and Podzun, R.: Sensitivity studies with the regional climate model REMO, Meteorology and Atmospheric Physics, 63, 119–129, https://doi.org/10.1007/BF01025368, 1997.

Janjic, Z. I., Gerrity, J. P., and Nickovic, S.: An alternative approach to nonhydrostatic modeling, Monthly Weather Review, 129, 1164–1178, https://doi.org/10.1175/1520-0493(2001)129<1164:AAATNM>2.0.CO;2, 2001.

Kadow, C., Illing, S., Lucio-Eceiza, E., Bergemann, M., Ramadoss, M., Sommer, P., Kunst, O., Schartner, T., Pankatz, K., Grieger, J., Schuster, M., Richling, A., Thiemann, H., Kirchner, I., Rust, H., Ludwig, T., Cubasch, U., and Ulbrich, U.: Introduction to Freva - A Free Evaluation System Framework for Earth System Modeling, Journal of Open Research Software, 9, https://doi.org/10.5334/jors.253, 2021.

Kaspar, F., Müller-Westermeier, G., Penda, E., Mächel, H., Zimmermann, K., Kaiser-Weiss, A., and Deutschländer, T.: Monitoring of climate change in Germany – data, products and services of Germany's National Climate Data Centre, Advances in Science and Research, 10, 99–106, https://doi.org/10.5194/asr-10-99-2013, 2013.

Kaspar, F., Imbery, F., and Friedrich, K.: Nutzung klimatologischer Referenzperioden ab 2021, Tech. rep., Deutscher Wetterdienst, https://www.dwd.de/DE/leistungen/besondereereignisse/verschiedenes/20210119_neue_referenzperiode.pdf?__blob=publicationFile&v=6, 2021.

Kendon, E. J., Prein, A. F., Senior, C. A., and Stirling, A.: Challenges and outlook for convection-permitting climate modelling, Philosophical Transactions of the Royal Society A: Mathematical, Physical and Engineering Sciences, 379, 20190 547, https://doi.org/10.1098/rsta.2019.0547, 2021.

Kotlarski, S., Keuler, K., Christensen, O. B., Colette, A., Déqué, M., Gobiet, A., Goergen, K., Jacob, D., Lüthi, D., Van Meijgaard, E., Nikulin, G., Schär, C., Teichmann, C., Vautard, R., Warrach-Sagi, K., and Wulfmeyer, V.: Regional climate modeling on European scales: a joint standard evaluation of the EURO-CORDEX RCM ensemble, Geoscientific Model Development, 7, 1297–1333, https://doi.org/10.5194/gmd-7-1297-2014, 2014.

Krähenmann, S., Walter, A., Brienen, S., Imbery, F., and Matzarakis, A.: Monthly, daily and hourly grids of 12 commonly used meteorological variables for Germany estimated by the Project TRY Advancement, https://doi.org/10.5676/DWD_CDC/TRY_BASIS_V001, 2016.

Kreklow, J., Tetzlaff, B., Burkhard, B., and Kuhnt, G.: Radar-Based Precipitation Climatology in Germany-Developments, Uncertainties and Potentials, Atmosphere, 11, 217, https://doi.org/10.3390/atmos11020217, 2020.

Lanzante, J. R., Dixon, K. W., Nath, M. J., Whitlock, C. E., and Adams-Smith, D.: Some pitfalls in statistical downscaling of future climate, Bulletin of the American Meteorological Society, 99, 791–803, https://doi.org/10.1175/BAMS-D-17-0046.1, 2018.

Lucas-Picher, P., Argüeso, D., Brisson, E., Tramblay, Y., Berg, P., Lemonsu, A., Kotlarski, S., and Caillaud, C.: Convection-permitting modeling with regional climate models: Latest developments and next steps, Wiley Interdisciplinary Reviews: Climate Change, 12, e731, https://doi.org/10.1002/wcc.731, 2021.

https://doi.org/10.5194/egusphere-2026-1024
Preprint. Discussion started: 10 June 2026

Ludwig, P., Ehmele, F., Franca, M. J., Mohr, S., Caldas-Alvarez, A., Daniell, J. E., Ehret, U., Feldmann, H., Hundhausen, M., Knippertz, P., Küpfer, K., Kunz, M., Mühr, B., Pinto, J. G., Quinting, J., Schäfer, A. M., Seidel, F., and Wisotzky, C.: A multi-disciplinary analysis of the exceptional flood event of July 2021 in central Europe – Part 2: Historical context and relation to climate change, Natural Hazards and Earth System Sciences, 23, 1287–1311, https://doi.org/10.5194/nhess-23-1287-2023, 2023.

Maraun, D., Widmann, M., Gutiérrez, J. M., Kotlarski, S., Chandler, R. E., Hertig, E., Wibig, J., Huth, R., and Wilcke, R. A. I.: VALUE: A framework to validate downscaling approaches for climate change studies, Earth's Future, 3, 1–14, https://doi.org/10.1002/2014EF000259, 2015.

Measham, T. G., Preston, B. L., Smith, T. F., Brooke, C., Gorddard, R., Withycombe, G., and Morrison, C.: Adapting to climate change through local municipal planning: barriers and challenges, Mitigation and Adaptation Strategies for Global Change, 16, 889–909, https://doi.org/10.1007/s11027-011-9301-2, 2011.

Mironov, D., Ritter, B., Schulz, J.-P., Buchhold, M., Lange, M., and Machulskaya, E.: Parameterisation of sea and lake ice in numerical weather prediction models of the German Weather Service, Tellus A, 64, https://doi.org/10.3402/tellusa.v64i0.17330, 2012.

Mironov, D. V.: Parameterization of lakes in numerical weather prediction. Description of a lake model, Tech. Rep. 11, Consortium for Small-Scale Modelling, https://doi.org/10.5676/DWD_pub/nwv/cosmo-tr_11, 2008.

Mohr, S., Ehret, U., Kunz, M., Ludwig, P., Caldas-Alvarez, A., Daniell, J. E., Ehmele, F., Feldmann, H., Franca, M. J., Gattke, C., Hundhausen, M., Knippertz, P., Küpfer, K., Mühr, B., Pinto, J. G., Quinting, J., Schäfer, A. M., Scheibel, M., Seidel, F., and Wisotzky, C.: A multi-disciplinary analysis of the exceptional flood event of July 2021 in central Europe – Part 1: Event description and analysis, Natural Hazards and Earth System Sciences, 23, 525–551, https://doi.org/10.5194/nhess-23-525-2023, 2023.

Molina, M. O., Careto, J. M., Gutiérrez, C., Sánchez, E., Goergen, K., Sobolowski, S., Coppola, E., Pichelli, E., Ban, N., Belušić, D., Short, C., Caillaud, C., Dobler, A., Hodnebrog, Ø., Kartsios, S., Lenderink, G., de Vries, H., Göktürk, O., Milovac, J., Feldmann, H., Truhetz, H., Demory, M. E., Warrach-Sagi, K., Keuler, K., Adinolfi, M., Raffa, M., Tölle, M., Sieck, K., Bastin, S., and Soares, P. M. M.: The added value of simulated near-surface wind speed over the Alps from a km-scale multimodel ensemble, Climate Dynamics, 62, 4697–4715, https://doi.org/10.1007/s00382-024-07257-4, 2024.

Perkins, S. E., Pitman, A. J., Holbrook, N. J., and McAneney, J.: Evaluation of the AR4 climate models' simulated daily maximum temperature, minimum temperature, and precipitation over Australia using probability density functions, Journal of Climate, 20, 4356–4376, https://doi.org/10.1175/JCLI4253.1, 2007.

Pfeifroth, U., Kothe, S., Drücke, J., Trentmann, J., Schröder, M., Selbach, N., and Hollmann, R.: Surface Radiation Data Set - Heliosat (SARAH) - Edition 3, https://doi.org/10.5676/EUM_SAF_CM/SARAH/V003, 2023.

Pietikäinen, J.-P., Sieck, K., Buntemeyer, L., Frisius, T., Nam, C., Hoffmann, P., Pop, C., Rechid, D., and Jacob, D.: REMO2020: A Modernised Modular Regional Climate Model, Geoscientific Model Development, 18, 7907–7949, https://doi.org/10.5194/gmd-18-7907-2025, 2025.

Pinto, J. G., Hundhausen, M., Weber, A., Kohlhepp, R., Mihalyfi-Dean, C., Schipper, J. W., and Feldmann, H.: User-relevant climate indices and associated uncertainties from transient convection-permitting climate model projections, International Journal of Climatology, 46, https://doi.org/10.1002/joc.70304, 2026.

Prein, A. F., Langhans, W., Fosser, G., Ferrone, A., Ban, N., Goergen, K., Keller, M., Tölle, M., Gutjahr, O., Feser, F., Brisson, E., Kollet, S., Schmidli, J., van Lipzig, N. P. M., and Leung, R.: A review on regional convection-permitting climate modeling: Demonstrations, prospects, and challenges, Reviews of Geophysics, 53, 323–361, https://doi.org/10.1002/2014RG000475, 2015.

https://doi.org/10.5194/egusphere-2026-1024
Preprint. Discussion started: 10 June 2026

Prill, F., Reinert, D., Rieger, D., and Zaengel, G.: ICON Tutorial: Working with the ICON Model, Tech. rep., Deutscher Wetterdienst, Karlsruhe Institute of Technology, Max-Planck-Institut fuer Meteorologie, https://doi.org/10.5676/DWD_pub/nwv/icon_tutorial2023, 2023.

Raschendorfer, M.: The new turbulence parameterization of LM, in: COSMO News Letter No. 1, Consortium for Small-Scale Modelling, edited by Doms, G. and Schättler, U., pp. 25–28, Deutscher Wetterdienst, Offenbach am Main, Germany, https://www.cosmo-model.org/content/model/documentation/newsLetters/newsLetter01/newsLetter_01.pdf, 2008.

Rauthe, M., Steiner, H., Riediger, U., Mazurkiewicz, A., and Gratzki, A.: A Central European precipitation climatology – Part I: Generation and validation of a high-resolution gridded daily data set (HYRAS), Meteorologische Zeitschrift, 22, 235–256, https://doi.org/10.1127/0941-2948/2013/0436, 2013.

Razafimaharo, C., Krähemann, S., Höpp, S., Rauthe, M., and Deutschländer, T.: New high-resolution gridded dataset of daily mean, minimum, and maximum temperature and relative humidity for Central Europe (HYRAS), Theoretical and Applied Climatology, 142, 1531–1553, https://doi.org/10.1007/s00704-020-03388-w, 2020.

Reyers, M., Pinto, J. G., and Moemken, J.: Statistical-dynamical downscaling for wind energy potentials: evaluation and applications to decadal hindcasts and climate change projections, International Journal of Climatology, 35, 229–244, https://doi.org/10.1002/joc.3975, 2015.

Rockel, B. and Geyer, B.: COSMO-CLM Starter Package, https://doi.org/10.5281/zenodo.7290478, 2022a.

Rockel, B. and Geyer, B.: SPICE (Starter Package for ICON-CLM Experiments), https://doi.org/10.5281/zenodo.6838984, 2022b.

Rockel, B., Will, A., and Hense, A.: The regional climate model COSMO-CLM (CCLM), Meteorologische Zeitschrift, 17, 347–348, https://doi.org/10.1127/0941-2948/2008/0309, 2008.

Rousi, E., Fink, A. H., Andersen, L. S., Becker, F. N., Beobide-Arsuaga, G., Breil, M., Cozzi, G., Heinke, J., Jach, L., Niermann, D., Petrovic, D., Richling, A., Riebold, J., Steidl, S., Suarez-Gutierrez, L., Tradowsky, J. S., Coumou, D., Düsterhus, A., Ellsäßer, F., Fragkoulidis, G., Gliksman, D., Handorf, D., Haustein, K., Kornhuber, K., Kunstmann, H., Pinto, J. G., Warrach-Sagi, K., and Xoplaki, E.: The extremely hot and dry 2018 summer in central and northern Europe from a multi-faceted weather and climate perspective, Natural Hazards and Earth System Sciences, 23, 1699–1718, https://doi.org/10.5194/nhess-23-1699-2023, 2023.

Schrodin, P. and Heise, E.: The Multi-Layer Version of the DWD Soil Model TERRA_LM, Tech. Rep. 2, Consortium for Small-Scale Modelling, https://doi.org/10.5676/DWD_pub/nwv/cosmo-tr_2, 2001.

Schulz, J.-P. and Vogel, G.: Improving the Processes in the Land Surface Scheme TERRA: Bare Soil Evaporation and Skin Temperature, Atmosphere, 11, https://doi.org/10.3390/atmos11050513, 2020.

Schulz, J.-P., Vogel, G., Becker, C., Kothe, S., Rummel, U., and Ahrens, B.: Evaluation of the ground heat flux simulated by a multi-layer land surface scheme using high-quality observations at grass land and bare soil, Meteorologische Zeitschrift, 25, 607–620, https://doi.org/10.1127/metz/2016/0537, 2016.

Schulzweida, U.: CDO User Guide, https://doi.org/10.5281/zenodo.7112925, 2022.

Seifert, A.: A revised cloud microphysical parameterization for COSMO-LME, in: COSMO News Letter No. 7, Proceedings from the 8th COSMO General Meeting in Bucharest, edited by Schaettler, U., Montani, A., and Milelli, M., pp. 25–28, Deutscher Wetterdienst, Offenbach am Main, Germany, https://www.cosmo-model.org/content/model/documentation/newsLetters, 2008.

Soares, P. M. M., Careto, J. A. M., Cardoso, R. M., Goergen, K., Katragkou, E., Sobolowski, S., Coppola, E., Ban, N., Belušić, D., Berthou, S., Caillaud, C., Dobler, A., Hodnebrog, Ø., Kartsios, S., Lenderink, G., Lorenz, T., Milovac, J., Feldmann, H., Pichelli, E., Truhetz, H., Demory, M. E., de Vries, H., Warrach-Sagi, K., Keuler, K., Raffa, M., Tölle, M., Sieck, K., and Bastin, S.: The added value of km-scale

https://doi.org/10.5194/egusphere-2026-1024
Preprint. Discussion started: 10 June 2026

simulations to describe temperature over complex orography: the CORDEX FPS-Convection multi-model ensemble runs over the Alps, Climate Dynamics, 62, 4491–4514, https://doi.org/10.1007/s00382-022-06593-7, 2024.

Stevens, B., Satoh, M., Auger, L., Biercamp, J., Bretherton, C. S., Chen, X., Düben, P., Judt, F., Khairoutdinov, M., Klocke, D., Kodama, C., Kornblueh, L., Lin, S.-J., Neumann, P., Putman, W. M., Röber, N., Shibuya, R., Vanniere, B., Vidale, P. L., Wedi, N., and Zhou, L.: DYAMOND: the DYnamics of the Atmospheric general circulation Modeled On Non-hydrostatic Domains, Progress in Earth and Planetary Science, 6, 61, https://doi.org/10.1186/s40645-019-0304-z, 2019.

Tiedtke, M.: A comprehensive mass flux scheme for cumulus parameterization in large-scale models, Monthly Weather Review, 117, 1779–1800, https://doi.org/10.1175/1520-0493(1989)117<1779:ACMFSF>2.0.CO;2, 1989.

Van Pham, T., Steger, C., Rockel, B., Keuler, K., Kirchner, I., Mertens, M., Rieger, D., Zaengl, G., and Frueh, B.: ICON in Climate Limited-area Mode (ICON release version 2.6.1): a new regional climate model, Geoscientific Model Development, 14, 985–1005, https://doi.org/10.5194/gmd-14-985-2021, 2021.

Vautard, R., Gobiet, A., Sobolowski, S., Kjellström, E., Stegehuis, A., Watkiss, P., Mendlik, T., Landgren, O., Nikulin, G., Teichmann, C., and Jacob, D.: The European climate under a 2 C global warming, Environmental Research Letters, 9, 034 006, https://doi.org/10.1088/1748-9326/9/3/034006, 2014.

Williams, P. D.: A Proposed Modification to the Robert-Asselin Time Filter, Monthly Weather Review, 137, 2538–2546, https://doi.org/10.1175/2009MWR2724.1, 2009.

Winterrath, T., Brendel, C., Hafer, M., Junghänel, T., Klameth, A., Lengfeld, K., Walawender, E., Weigl, E., and Becker, A.: Radar climatology (RADKLIM) version 2017.002; gridded precipitation data for Germany, https://doi.org/10.5676/DWD/RADKLIM_RW_V2017.002, 2018.

Zängl, G., Reinert, D., Ripodas, P., and Baldauf, M.: The ICON (ICOsahedral Non-hydrostatic) modelling framework of DWD and MPI-M: Description of the non-hydrostatic dynamical core, Quarterly Journal of the Royal Meteorological Society, 141, 563–579, https://doi.org/10.1002/qj.2378, 2015.